www.coinweb.no

SINTEF Building and Infrastructure Hedda Vikan and Stefan Jacobsen (NTNU)

Influence of rheology on the pumpability of mortar

COIN Project report 21 - 2010

SINTEF

SINTEF Building and Infrastructure

Hedda Vikan and Stefan Jacobsen

Influence of rheology on the pumpability of mortar

P 2 Improved construction technology

SP 2.4 Workability

COIN Project report 21 – 2010

COIN Project report no 21
Hedda Vikan and Stefan Jacobsen (NTNU)
Influence of rheology on the pumpability of mortar

P 2 Improved construction technology
SP 2.4 Workability

Keywords:
Concrete, rheology, pumping

Photo, cover: «Stairs, House of Gyldendahl»(www.gyldendal.no)

ISSN 1891–1978 (online)
ISBN 978-82-536-1158-7 (pdf)

Address: Forskningsveien 3 B
POBox 124 Blindern
N-0314 OSLO
Tel: +47 22 96 55 55
Fax: +47 22 69 94 38 and 22 96 55 08

www.sintef.no/byggforsk
www.coinweb.no

Cooperation partners / Consortium Concrete Innovation Centre (COIN)

Aker Solutions
Contact: Jan-Diederik Advocaat
Email: jan-diederik.advocaat@akersolutions.com
Tel: +47 67595050

Saint Gobain Weber
Contact: Geir Norden
Email: geir.norden@saint-gobain.com
Tel: +47 22887700

Norcem AS
Contact: Terje Rønning
Email: terje.ronning@norcem.no
Tel: +47 35572000

NTNU
Contact: Terje Kanstad
Email: terje.kanstad@ntnu.no
Tel: +47 73594700

Rescon Mapei AS
Contact: Trond Hagerud
Email: trond.hagerud@resconmapei.no
Tel: +47 69972000

SINTEF Building and Infrastructure
Contact: Tor Arne Hammer
Email: tor.hammer@sintef.no
Tel: +47 73596856

Skanska Norge AS
Contact: Sverre Smeplass
Email: sverre.smeplass@skanska.no
Tel: +47 40013660

Spenncon AS
Contact: Ingrid Dahl Hovland
Email: ingrid.dahl.hovland@spenncon.no
Tel: +47 67573900

Norwegian Public Roads Administration
Contact: Kjersti K. Dunham
Email: kjersti.kvalheim.dunham@vegvesen.no
Tel: +47 22073940

Unicon AS
Contact: Stein Tosterud
Email: stto@unicon.no
Tel: +47 22309035

Veidekke Entreprenør ASA
Contact: Christine Hauck
Email: christine.hauck@veidekke.no
Tel: +47 21055000

Preface

This study has been carried out within COIN - Concrete Innovation Centre - one of presently 14 Centres for Research based Innovation (CRI), which is an initiative by the Research Council of Norway. The main objective for the CRIs is to enhance the capability of the business sector to innovate by focusing on long-term research based on forging close alliances between research-intensive enterprises and prominent research groups.

The vision of COIN is creation of more attractive concrete buildings and constructions. Attractiveness implies aesthetics, functionality, sustainability, energy efficiency, indoor climate, industrialized construction, improved work environment, and cost efficiency during the whole service life. The primary goal is to fulfil this vision by bringing the development a major leap forward by more fundamental understanding of the mechanisms in order to develop advanced materials, efficient construction techniques and new design concepts combined with more environmentally friendly material production.

The corporate partners are leading multinational companies in the cement and building industry and the aim of COIN is to increase their value creation and strengthen their research activities in Norway. Our over-all ambition is to establish COIN as the display window for concrete innovation in Europe.

About 25 researchers from SINTEF (host), the Norwegian University of Science and Technology - NTNU (research partner) and industry partners, 15 - 20 PhD-students, 5 - 10 MSc-students every year and a number of international guest researchers, work on presently 8 projects in three focus area:

- Environmentally friendly concrete
- Economically competitive construction
- Technical performance

COIN has presently a budget of NOK 200 mill over 8 years (from 2007), and is financed by the Research Council of Norway (approx. 40 %), industrial partners (approx 45 %) and by SINTEF Building and Infrastructure and NTNU (in all approx 15 %).

For more information, see www.coinweb.no

Tor Arne Hammer
Centre Manager

Summary

The rheological and material parameters determining the pumpability of fresh self-compacting mortar have been studied. A full-scale set up with 70 meter long 50 mm diameter rubber hoses fed by a screw pump was used. The pump delivered a constant concrete flow rate and pressure for a given pumping frequency, hose diameter and – length with a maximum capacity of 7 m^3/h. The concrete pressure gradient over the hose length (dp/dx) and flow rate were measured to quantify pumpability. The rheological properties of the pumped mortars were measured with a ConTec BML viscometer. Finally, the rheological properties of the slip layer that occurs in vicinity of the wall of the hose during pumping was simulated by studying the matrix phase (paste and filler < 0.125 mm) with a parallel plate rheometer.

Five different concrete mixes were investigated showing that slump flow is not suitable for differentiating pumpability. Interpretation of rheological data was, moreover, complicated since the measured values of plastic viscosity and yield stress were altered simultaneously from mix to mix.

The data imply that both yield stress and plastic viscosity govern pumpability. Increased plastic viscosity of mortar and paste was found to correlate with decreased mortar pumpability. No clear trends could be found for mortar yield stress. Increased paste yield stress was, however surprisingly, related to increased pumpability. The plastic viscosity seemed, however, to dominate yield stress when the two factors varied simultaneously within the given workability range. These parameters should, therefore, not be studied independently. Increased hysteresis area calculated from the paste measurements correlated well with reduced pump flow, also indicating a relation to the rheology of the slip layer.

The predicted pressure losses were 5-7 times higher than the measured values. This indicates that one or more of the premises of the Buckingham-Reiner equation are erroneous. We suspect that inhomogeneous fluid and slippage at the pipe walls are main factors. The effect of plug and slip layer was therefore investigated in detail.

The existence of a plug was based on yield stress measured both in matrix and mortar. Gel-strength tests in the parallel plate viscometer correlated well to the matrix yield for the 5 final mixes studied. The combination of instrumented steady state pumping, parallel plate viscometer and visualized boundary flow rate were all used to estimate slip layer thickness. The modified Buckingham Reiner equation resulted in slip zone thickness in the order of 0.6 – 1 mm. The calculated slip layer thicknesses were not very sensitive to variations in matrix yield stress, whereas plastic viscosity had a major effect as shown in plots of slip zone viscosity vs slip zone thickness. At the slip zone thickness corresponding to the matrix rheology, the calculated specific viscosities (Pa·s/m) were all similar to the lowest values reported by Kaplan (2001). The average rates of shear in the thinnest slip zone were estimated to be as high as 1000 [s^{-1}]. This is much higher than those used in the parallel plate viscometer [100 s^{-1}] and future parallel plate viscometre test made in conjunction with studies of this kind should be carried out to 1000 [s^{-1}].

Based on a few flow profile calculations and comparison with visualized profiles it seems reasonable to assume that the rheological properties of the concrete are not constant, but vary over the cross section of the tube and possibly also along the tube due to factors such as tixotropic behaviour, possibly shear thickening, stiffening, wall effects and/or segregation under shear.

Some investigations of effect of pumping on compressive strength were made by measuring strength on cubes made from concrete before and after pumping. These showed negligible effects of pumping on strength.

The research described in this report should be complemented with additional tests including mortars with a wider workability range and more systematic variation of yield stress and plastic viscosity. Further research should also include studies of the influence of pump type (piston and screw pump) on the correlations between rheological properties of pumped materials and pumpability. Larger pumps will, moreover, enable pumping of concretes with larger aggregate size than 8 mm as used in this study. It is accordingly recommended to study the influence of aggregate size on pumpability.

An extensive preliminary study has been performed on the free flow profile (not pumped, but flowing due to gravitational forces) of coloured mortars. The results have shown that the type of tube material in which the mortar is flowing is of importance to the flow profiles. Full-scale pumping experiments with different tube materials should therefore be conducted, as well as full scale formwork filling.

Continued research on basic mechanisms of rheology as well as pumping and form filling experiments for various stable Self Compacting Concrete (SCC) with investigations of form filling and surface eveness should be performed.

Table of contents

1 Introduction

1.1 Principal objectives and scope

The principal objectives and the scope of the study have been to obtain a clearer knowledge about the main material and rheological parameters that govern the pumpability of self-compacting concrete. On site concrete pumping in Norway is often operated by the concrete truck driver. From discussions with concrete producers there seems to be a tendency that these pump operators have a bearing on the composition of the concrete by preferring richer mixes for pumping. From the cited literature study we know that increased cement content is certainly not the only way of ensuring appropriate pumpability. Furthermore, such a practice may give problems with economy, technology and environment due to high cost, increased heat of curing and shrinkage as well as unnecessarily high cement content.

We have investigated the relationship between the rheological properties of matrix and the pumpability of the concrete or mortar mix. Rheological measurements on paste are less time- and material consuming than full-scale measurements on mortar. Furthermore, the flow of concrete through a pipe might seem a quite simple and well defined case of flow. If we manage to understand this well then related topics such as form filling and flow along surfaces as affected by concrete rheology and surface properties could also be improved.

1.2 Background

The pumpability of concrete can be defined as its ability to flow through pipes and hoses by the help of a pump while maintaining its fresh and hardened properties (ACI 1998, Jolin et al. 2006).

Contradictory reports have been given about the influence of various rheological parameters on the concrete pumpability. Pumpability of traditionally vibrated concrete is generally found to increase with increasing workability (Sakuta et al. 1989). On high slump high performance concrete, HPC, Hansen (1988) reported that both yield strength and plastic viscosity, ,measured as g and h with Tattersalls original Mk II apparatus (Tattersall and Banfill 1983), related to hydraulic oil pressure in a single piston pump. The best correlation was given by the yield stress. Hu and de Larrard (1996) reported, on the other hand, that plastic viscosity correlated to pumpability in high slump high performance concrete. They quantified pumpability as the ratio between the pump cylinder pressure and the number of strokes per minute [(bar·min)/stroke], whereas rheology was measured with their BTRHEOM viscometer. Parallel measurements of yield stress, slump and spread did not correlate to pumpability.

Feys et al. (2008) reports that higher pressure losses, and thus higher shear stresses, are measured for self-compacting concrete (SCC) than for traditionally vibrated concrete. The authors explained this by SCC having a higher viscosity than traditional concrete. They deduced that the plastic viscosity is the main rheological parameter influencing the pumpability.

An overview of the literature on pumping of concrete has been given in a previous study (Jacobsen et al. 2008). The report aimed to identify the relationship between pumpability and the properties of fresh mortar and concrete. A lowest possible pressure gradient, dp/dx, over the pump line in a specific pump set up for a given flow was found to be one way of quantifying the pumpability of different concrete mixes. Pumpability could then simply be quantified as the ratio (flow/pressure drop). Laboratory investigations indicated that at approximately constant pump flow (v_x) the pressure drop (dp/dx) relates to plastic viscosity (μ) of the pumped concrete measured with the BML viscometer. The relation between dp/dx and yield stress (τ_y) was less clear.

It has been observed during pumping that the concrete in the vicinity of the tube wall is not the same as the bulk material (Tattersall and Banfill 1983, Kaplan 2001, Haist and Muller 2005, Kaplan et al. 2005). There could be several reasons for the formation of this paste- or matrix rich slip layer near the wall, one being the so-called "wall effect". The wall effect causes reduced packing of aggregate within a distance equal to half the maximum aggregate size from the pipe wall and thus increased paste content. Another effect is the granular nature of concrete causing dynamic segregation, possibly due to the tendency of rotating particles to move towards lower shear rate away from the wall (Thrane 2007). The pressure loss occurring through the hose during pumping has been related to the shear stresses of this layer (Kaplan et al. 2005). Kaplan (2001) reported that pumpability related to the plastic viscosity in the slip zone measured with a tribometer and based on assumptions on the thickness of the layer. The correlation between the slip zone viscosity and the plastic viscosity of the bulk concrete was however weak. It is natural to assume that the composition of the slip layer, and thus its rheological properties, is similar to the paste or the matrix (paste and filler) of the concrete. Kaplan et al. (2001, 2005) investigated the slip layer by use of a tribometer. A tribometer can in principle be constructed from a normal rheometer simply by constructing the stator and rotor of the rheometer in a way that allows slippage (i.e. smooth surfaces) or by using the same material as the inside of the pipes used for pumping. The specific slip layer viscosity of Kaplan et al. (2001, 2005) has the unit Pa·s/m. Observations and / or assumptions must therefore be made on the slip layer thickness.

1.3 Rheological models used in the study

1.3.1 Models used for paste and matrix

Numerous rheological models have been proposed to describe the rheology of cementitious materials. The Bingham model has become very popular due to its simplicity and ability to describe cementitious flow. The model describes the shear stress (τ) as a function of yield stress (τ_y), plastic viscosity (μ_p) and shear rate ($\dot{\gamma}$) as follows:

$$\tau = \tau_y + \mu_p \cdot \dot{\gamma} \tag{1}$$

The model is used throughout this study both for matrix and paste since this is the standard model of the BML-viscometer for mortar and concrete and it is very easy to calculate from the data of the parallel plate viscometer used for paste and matrix. (Note that we define matrix as paste and all particles < 0,125 mm.) The yield stress is calculated from the down-curve by using the regression line for shear rate range 100-1 s^{-1}.

Several of the pastes and matrices made in this study had shear thinning or shear thickening behaviour. The Herschel-Bulkley model has therefore also been used in addition to the Bingham model. The Herschel-Bulkley model is given by equation (2) were τ_y is a yield stress parameter; K is the "consistency" [Pa·s^n] and n is the power law index.

$$\tau = \tau_y + K \cdot \dot{\gamma}^n \tag{2}$$

The yield stress and plastic viscosity of shear thinning or shear thickening materials depends on the applied shear rate range. It will also be shown in the following chapters that eq. (2) can result in negative yield stresses for pastes with high degree of workability. A negative yield stress has no physical meaning.

There has been raised a question whether or not a yield stress exists or whether all non-Newtonian materials will exhibit a finite zero-shear viscosity. Barnes and Walters (1985)

states that the yield stress concept is an idealization and that given accurate measurements, no yield stress exists. They claim that even concentrated systems flow in the limit of very low stresses and that these materials appear not to flow merely because the zero shear viscosity is so high. Yahia and Khayat (2001) support this statement by finding that the yield stress correlated well to the apparent viscosity at low shear rate (5 s^{-1}).

As well as describing the flow curve with the usual Bingham and Herschel-Bulkley models, we chose to investigate gel-strength (i.e. yield stress from rest) and the areas under the experimental shear stress-shear rate curves (Pa/s, equal to applied work W/m^3) as a measure of "flow resistance" of paste as described by Vikan et al. (2005). A shear rate range of 21.5 - 4.42 s^{-1} has been used for the calculations.

Thixotropy has also been studied. Thixotropy is defined as a gradual decrease of the viscosity under shear stress followed by a gradual recovery of structure when the stress is removed (Barnes et al. 1989). The rheological measurement sequence as well as the material itself will influence the thixotropic properties. Thixotropy has in this study been quantified by calculating the hysteresis areas defined between the rheological up- and down curves measured on paste, Vikan (2005)

1.3.2 Models used for calculation of flow

Laminar flow in pipes can generally be considered as flow with straight, parallel streamlines. The flow is driven by the pressure gradient and the gravity. Assumptions are as follows:

- The fluid is incompressible and homogeneous
- The flow is one-dimensional, with no radial or tangential flow component
- The flow is steady and laminar
- No slippage at the walls

The mechanical equilibrium of a cylindrical element of generalized fluid is as follows:

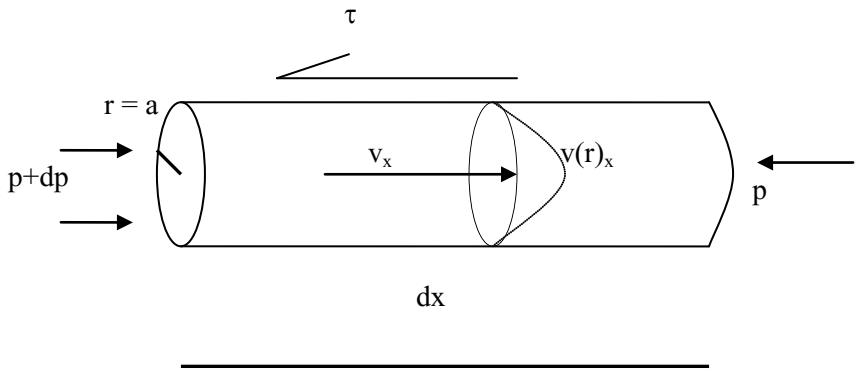

Figure 1: Simplified cylindrical element with uni-axial pressure difference

where:

p: pressure [Pa]
x: length [m]
v_x: mean concrete flow [m/s]
v(r): concrete flow as function of radius, flow profile [m/s]
a: radius of pipe [m]
τ: interface shear stress [Pa]

Mechanical equilibrium along the x-axis of the pipe element in Figure 1 requires: $\Sigma F_x = 0$:

$$\pi r^2 dp - \tau 2\pi r dx = 0 \tag{4}$$

Bingham fluid

For a Bingham fluid the cylindrical volume element can only start to move in a tube when the shear-stress $\tau > \tau_y$. For a no-slip condition this means that the cylindrical element in Figure 1 will start to move near the pipe wall like a plug with radius R_p since the resulting shear load will be largest there, see Figure 2.

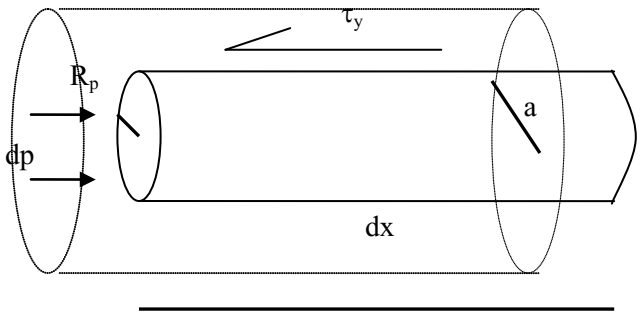

Figure 2: Plug with radius R_p as shear load from pump pressure exceeds the yield τ_y.

Combining equation (1) and (4) gives:

$$\pi r^2 dp - 2\pi r dx(\tau_y + \mu \frac{dv}{dr}) = 0 \tag{5}$$

The velocity distribution v(r) as the fluid flows through a pipe with radius a is found by separating and integrating (5) with the boundary condition v(a) = 0 (no slip):

$$v(r) = \int dv = \frac{1}{2\mu}\frac{dp}{dx}\int r dr - \frac{\tau_y}{\mu}\int dr \tag{6}$$

Mechanical equilibrium in the x-direction gives the radius of the plug, R_p (m):

$$\pi {R_p}^2 dp - 2\pi R_p dx \tau_y = 0 \Rightarrow R_p = \frac{2\tau_y}{(dp/dx)} \tag{7}$$

The integration of equation (6) must therefore give a flow distribution that includes the plug. With positive pressure gradient in the flow direction (6) becomes:

$$v(r) = \frac{(a^2 - r^2)}{4\mu}\frac{dp}{dx} - \frac{\tau_y}{\mu}(a - r) \qquad r \geq R_p$$

$$v(r) = v(R_p) \qquad r \geq R_p \tag{8}$$

Equation (8) does not allow any transport if $R_p \geq a$. If there is transport in such a case it is highly probable that the concrete is flowing through the pipe more or less like a plug with a lubricating slippage layer between the plug and the pipe wall. Here we shall treat this in a simplified manner by estimating the layer thickness and assuming that it has Bingham behaviour.

The total (integrated) flow, G_x [m^3/s] is obtained from (8) by multiplication of the plug contribution ($v(R_p)$) and integration of the rest of the cross section between the plug and the pipe wall ($v(R_p)$ to v(a)):

$$G_x = v(R_p)\pi R_p^2 + \int_{R_0}^{a}\left[\frac{(a^2-r^2)}{4\mu}\frac{dp}{dx} - \frac{\tau_y}{\mu}(a-r)\right]2\pi r\,dr \qquad (9)$$

The resulting total flow, the so-called *Buckingham-Reiner equation* (Tattersall and Banfill 1983) can, after integration and some algebra, be written (Kaplan 2001):

$$G_x = \frac{\pi a^4}{8\mu}\frac{dp}{dx}\left[1-\frac{4}{3}\left(\frac{2\tau_y}{a(dp/dx)}\right)+\frac{1}{3}\left(\frac{2\tau_y}{a(dp/dx)}\right)^4\right] = \frac{\pi a^4}{8\mu}\frac{dp}{dx}\left[1-\frac{4R_p}{3a}+\frac{1}{3}\left(\frac{R_p}{a}\right)^4\right] \qquad (10)$$

The plug radius, R_p is given by equation (7). The total volume flow, G_x [m^3/s]$_x$, and mean flow velocity v_x [m/s], are found from the velocity profile, v(r), and the area of the tube cross section:

$$dG_x = v\cdot dA = v(r)\cdot\left(2\pi r\cdot dr\right) \text{ and } v_x = \frac{1}{\pi a^2}G_x \qquad (11)$$

Equation (8) and (10) normally underestimate concrete flow. However, by evaluating R_p from equation (7) based on measurements and calculating the flow profiles and measuring total one can assess whether a concrete is far from, or close to plug flow.

The slip layer characteristics is one reason for the underestimation of flow of eq. (8) – (10) when using measured Bingham parameters and dp/dx measured during full scale pumping. Based on literature and our experiences with pumping- and flow experiments so far in COIN we suspect that factors like the rheology of the material in the slip layer (i.e. paste/matrix), its thickness and also the local microscopic conditions at the transition between fluid and pipe wall are of importance (slip, no slip or perhaps “degree of slip” of some kind).

Following the presentation of the experimental results we will present a simplified way of calculating slip layer thickness by fitting calculated flow to measured pump flow by letting the slip layer have different rheological properties from the concrete. This is motivated by observations in the parallel plate viscometer (Vikan et al (2009)) and of zero velocity at rubber pipe walls (Jacobsen et al (2009). From this we will use the rheological properties measured on the matrix in a procedure to fit the integrated flow of equation (8) to a flow profile with no slip boundary condition of the lubricating paste or matrix between the plug and the pipe wall.

2 Recipe development

The objective of the experiments described in the following was to further investigate the relation between rheology and pumpability of fresh mortar and concrete. As a preliminary working hypothesis it was assumed that the two rheological parameters yield stress and plastic viscosity correlate to, or are sufficient to quantify, pumpability of any concrete mix. If so, then experiments could be carried out on materials with such variations of yield and plastic viscosity that subsequent pumping experiments could reveal the most important rheological parameter affecting pumpability. Tests on a series of concretes with varying yield stress and plastic viscosity values could even give limiting or recommended values to obtain a specific pumpability quantified as pressure loss (dp/dx) for a specific pump set-up.

Therefore, we developed a set of recipes for mini-concretes with such variations of yield and plastic viscosity that subsequent pumping experiments hopefully could reveal which rheological parameter is the most significant for pumpability. Matrixes were firstly developed and then up-scaled to mortar assuming that the obtained variations in rheology of paste would result in large enough variations in the rheology of the up-scaled mortar. However, small adjustments were made on the final mortar recipes. The final matrix compositions were thus copied from the pumped mortars and their rheological properties determined again by a parallel plate rheometer. Pilot- or pre-mixes were made and studied in order to obtain pastes with as different rheological properties as possible. The paste recipes were used as basis for development of mortars (see Appendix 7 for more information).

Geiker et al (2002) investigated the relations between paste- and concrete rheology and found unique relations with plastic viscosity increasing in the order 5 - 15 times in concrete whereas yield increased 50 - > 100 times. If this holds for all materials then working with both paste and concrete is very useful for our purpose since valuable information may be obtained both about rheology relating to flow and slip conditions. Following the previous discussion on existence of slip layers, the rheological properties of concrete equivalent paste or matrix was investigated since it may be assumed to represent the material in the slip layer and thus possibly affecting the flow during pumping.

2.1 Paste

2.1.1 Materials and recipes

The following materials were used for the paste experiments:

- Portland cement of type CEM II/A-V (containing 20 % low lime fly ash)
- Silica fume (Elkem Microsilica Grade 940)
- Filler with a particle size smaller than 0.125 mm, retrieved from the granitic sand by sieving
- Superplasticizer (Glenium 151 with 15±1 % dry material)
- Viscosity modifying stabilizer (Sika Stabilizer 4R with ca. 5 % dry material)

All paste recipes are given in Table 1. Total volume per batch was 300 ml.

Table 1: Paste recipes. Percentages are given per cement weight.

Mix No.	w/b	Silica fume (%)	Filler (%)	Superplasticizer (%)	Stabilizer (%)
51	0.50	0.0	0.0	1.0	0
52	0.50	2.5	0.0	2.0	1
53	0.50	5.0	12.5	1.2	0
54	0.50	5.0	0.0	0.8	0
55	0.56	2.5	0.0	2.0	1

2.1.2 Mixing and rheological measurement program

A high shear blender, Braun Multiquick Pro (600 watt), set to intensity level 6 was used for mixing the pastes. The blending was performed by adding solids to the water and mix for ½ minute, resting for 5 minutes and blending again for 1 minute.

The rheological parameters of the paste were recorded by a parallel plate (1 mm gap, upper plate and lower plate serrated) rheometer MCR 300 from Physica. The rheometer temperature control was set to 20°C. The following measurement sequence started 15 min after water addition:

- 1 minute with constant shear rate ($\dot{\gamma}$) of 60 s^{-1} to stir up the paste
- Stress (≥) – shear rate ($\dot{\gamma}$) curve with linear sweep of $\dot{\gamma}$ from 1 up to 100 s^{-1} in 30 points lasting 6 seconds each
- Stress (≥) – shear rate ($\dot{\gamma}$) curve with linear sweep of $\dot{\gamma}$ from 100 down to 1 s^{-1} in 30 points lasting 6 seconds each
- 10 seconds resting
- Shear rate ($\dot{\gamma}$) - stress (≥) curve with logarithmic sweep of ≥ from 0.5-250 Pa in 30 points each lasting 5 seconds in order to measure the gel strength (static yield stress) after 10 seconds rest
- 10 minutes rest
- Shear rate ($\dot{\gamma}$) - stress (≥) curve with logarithmic sweep of ≥ from 0.5-250 Pa in 30 points each lasting 5 seconds in order to measure the gel strength (static yield stress) after 10 minutes rest

The measurement sequence is visualised in Figure 3.

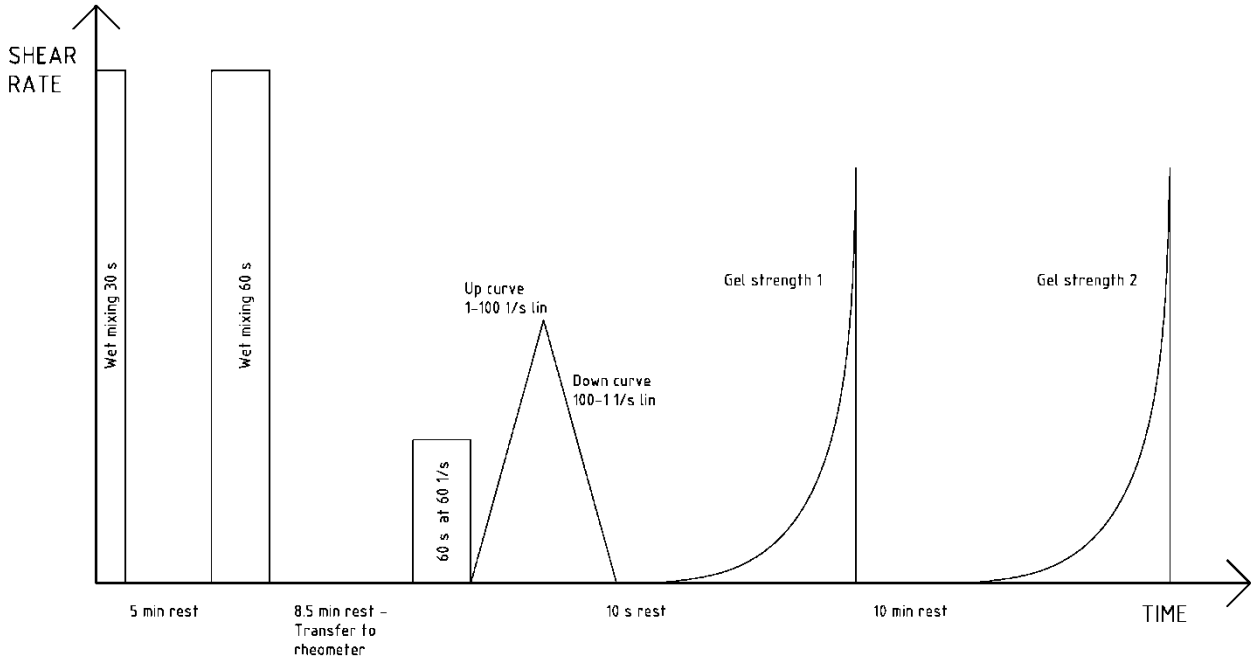

Figure 3: Schematic flow chart of the measurement sequence

2.1.3 Results

An overview of the rheological results is collected in Table 2 and Table 3. Flow curves can be found in appendix 0. The data show that the Herschel-Bulkley model renders excellent fits of the data. The model produces, however, in several cases negative yield stresses which have no physical meaning. This model will thus not be used further in this report for analysis of data.

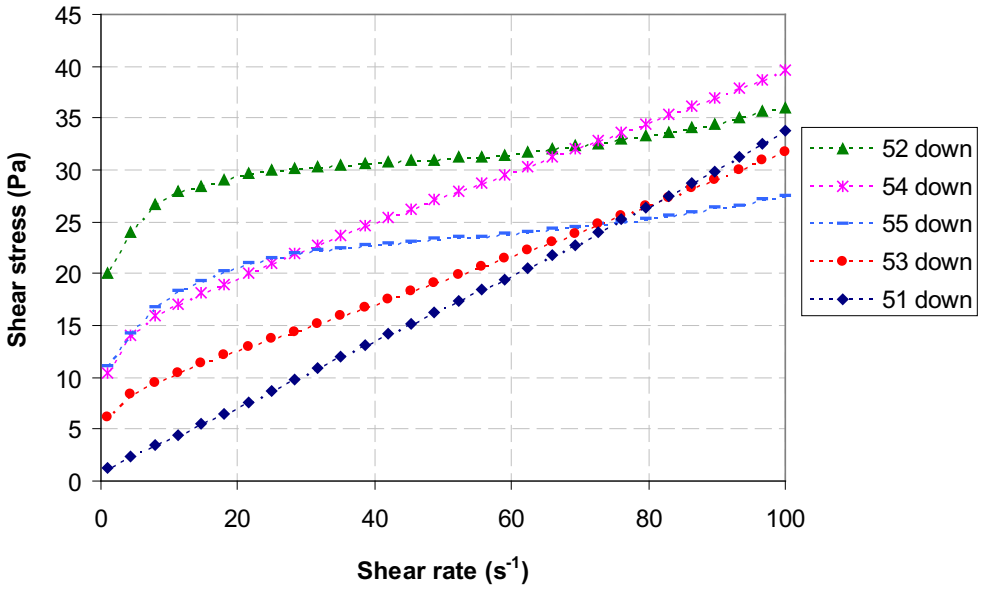

Figure 4: Rheological down curves measured for paste.

A series of pilot- or pre-mixes (described in Appendix A1) were prepared in order to obtain pastes with as different rheological properties as possible. That is, typically one paste with

high viscosity and high yield stress, one paste with high viscosity and low yield stress, one paste with low viscosity and low yield stress and last one paste with low viscosity and high yield stress. Mix 51-55 were a result of a combination of the tendencies observed by aid of the parallel plate rheometer for the pre-mixes, and at the same time a result of pastes that gave a pumpable fluid when combined with aggregates. As seen by the values in Table 2, a compromise is inevitable, and the great differences in rheological properties are overshadowed by the addition of aggregates. The rheological down-curves for these pastes are illustrated in Figure 4.

Table 2: Results – Bingham and Herschel-Bulkley parameters calculated on the whole shear rate range of the down curve (100-1 s^{-1}) for paste and matrix

Mix No.	Bingham Parameters			Herschel-Bulkley Parameters			
	τ_y	μ	R^2	τ_y	K	n	R^2
	[Pa]	[Pa·s]		[Pa]	[Pa·s]		
51	1	0.32	0.99	1.3	0.24	1.01	1.00
52	26	0.10	0.81	-6.8	27.33	0.09	0.95
53	7	0.24	1.00	7.0	0.30	0.96	1.00
54	14	0.26	0.99	11.0	0.88	0.75	1.00
55	17	0.11	0.82	-15.2	25.95	0.10	0.99

Table 3 shows the rheological properties of the matrix calculated as hysteresis area, flow resistance and gel strengths (Vikan 2005).

Table 3: Calculated hysteresis area, flow resistance and gel strengths measured on paste

Mix No.	Hysteresis Area	Flow Resistance	Gel strength 1	Gel strength 2
	[Pa/s]	[Pa/s]	[Pa]	[Pa]
51	310	86	0	6
52	254	475	41	50
53	337	185	7	11
54	342	298	14	14
55	190	315	21	27

In this study yield values of the pastes were determined in two ways. First yield was determined by regression of parallel plate viscometer runs with a set shear rate range of 100 to 1 s^{-1} assuming that the Bingham model applies. In addition, very small and stepwise increasing shear loads were applied from rest. The transition between elastic and plastic behaviour of fresh cement paste is registered as the so-called gel-strength (Vikan 2005).

At very small deformations from the applied shear load the start of viscous behaviour was observed from an initial elastic part for matrices 51-55. Figure 5 shows a plot of yield stress of the Bingham model applied to the down curves versus gel strength of the 5 final mixes investigated in this study (see Table 1). As can be seen there is a good correlation between yield stress deduced by the two different approaches for the 5 matrices. The gel strength is on average 1.6 times the Bingham yield stress. (Note that this result is not general and applicable to all cement based materials. When performing this plot for all material of this study the correlation was much weaker.

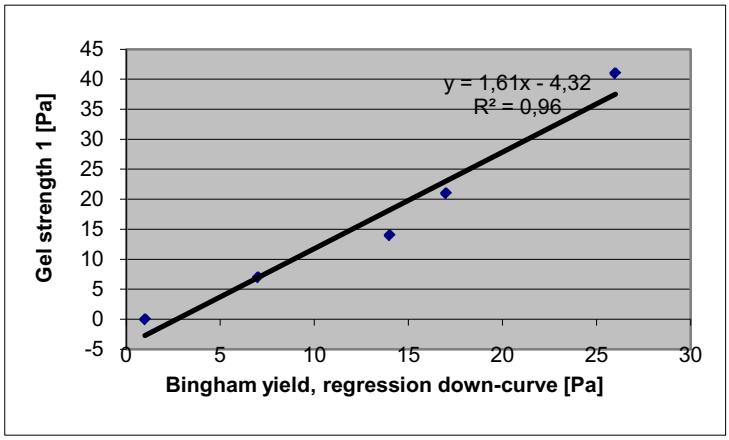

Figure 5: Correlation Gel strength versus yield stress determined by aid of the Bingham model for the matrices of mixes 51 – 55

In the gel-strength test the material shows viscous type behaviour at deformation rates beyond the apparent yield (or maximum yield stress reached before deformation rate, or rate of shear increases largely). Plots of the applied shear deformation and measured resulting shear stress reaction during the 5 seconds the actual deformation is applied (in the very sensitive instrument) will be proportional to load- deformation curves for an ideal elastic material according to Hooke's law:

$$\tau = G\gamma \tag{3}$$

In our measurements the shear modulus G is then proportional to the observed rate of change for the first measuring points where the shear rate intervals are approximately equal and the plots at the same time show (approximately) linear behaviour.

For the matrices used in the pump study and shown in figure 1 we mainly see linear elastic type of behaviour in the first part of the plot before the gel strength is reached (deformation $\gamma \geq 0 - 0{,}0001$ (rad)). The deformation intervals were approximately constant for each 5 sec load period and yield showed a quite linear increase. This observation is in line with the experiments by Billberg (2006) who measured the yield after some time of rest on concrete in a somewhat coarser way by use of the less accurate BML viscometer run at very low speed of rotation. Still he was able to detect the complete load deformation curve past the initial elastic part and into the plastic or visco-plastic and finally viscous region. In the initial part of loading of his concretes a drop of shear stress was observed and this is frequently seen in the gel-strength test.

3 Pumping tests

3.1 Experimental

3.1.1 Materials and recipes

The materials are identical to the ones given in Chapter 2.1.1. The mortars were added 1507 kg/m^3 0-8 mm granitic sand (corresponding to 66 wt%). Apart from that, their compositions were identical to the pastes.

The mixes were proportioned with 400 l/m^3 of matrix and with an estimation of 2 % air. 20 litre batches were mixed to be able to fill the test bucket of the BML (approximately 11 litres) and the slump cone. For most of the mixes, the 0-8 mm sand fraction was solely used. The 0-8 mm sand had a filler content (<125 µm) of 6.3%. The recipes of the mortars used for the full-scale pumping experiments are given by Table 4.

Table 4: Recipes of mortars. Percentages are given per cement weight.

	Mix				
	51	**52***	**53**	**54**	**55**
w/b	0.50	0.50	0.50	0.50	0.56
Superplasticizer (%)	1.0	2.0	1.2	0.8	2.0
Stabilizer (%)	0.0	1.0	0.0	0.0	1.0
Cement (kg/m^3)	494.5	480.1	442.2	468.1	448.3
Silica Fume (kg/m^3)	0.0	12.0	22.2	23.4	11.2
Filler (kg/m^3)	0.0	0.0	55.5	0.0	0.0
Sand (kg/m^3)	1507.4	1507.4	1507.4	1507.4	1507.4

*Not pumpable

3.1.2 Mixing of mortars for pumping tests

An Eirich laboratory batch mixer (counter current horizontal paddle mixer) with a maximum volume of 750 litres was used to prepare the mortar batches of 200 litres. The mixing cycle was as follows for trial mix 51 is given in Table 5. Small lumps of un-dispersed material was observed in mix 51.The initial dry mixing was therefore increased to 120 s for mix 52 - 54.

Table 5: Mixing sequence for mix 51. Initial dry mixing time was increased to 120 seconds for mix 52-55

Interval	**Duration** [s]	**Action**
1	0-60	Dry mixing
2	60-180	Wet mixing
3	180-300	Resting
4	300-540	Wet mixing
	Σ 9 min	

3.1.3 Experimental setup

The equipment for full-scale pumping tests consisted of an instrumented full scale pump circuit installed and developed in cooperation with maxit Group (now Weber). Several configurations of premix-silos, continuous and batch mixers, pumps, hose diameters and lengths are available. The following set up was used in this study:

- Screw (worm) pump, m-tec P30, with output of 7.5 kW and frequency control. The pump was tested for wearing before start. The stator was tightened, and water was pumped against a closed coupling The pump should be able to produce a pressure of 20 bar with this set-up according to the producer. If not, the stator is worn-out and should be replaced. The pump was able to produce 20 bar.
- The pump can handle a maximum aggregate size of 8 mm and had a maximum capacity of approximately 7 m^3/h at 50 Hz. Each mix was pumped at 25 and 50 Hz.
- 5 reinforced rubber hoses, each with a length of 13.3 m, and an internal diameter of 50 mm and 45 mm diameter at tapered joints were connected to a total length of 66.5 m. The hoses were identically positioned for all experiments (se Figure 6)
- 3 digital manometers of type IFM PF26 installed directly after the pump and after hose 1 and 2, i.e. at 13.3 and 26.6 m from the pump (a fourth manometer failed during testing)
- Ampere meter (data not applied in this study)
- Load cell with 60 litre plastic bag in a bucket to measure the mortar flow rate (kg/s converted to velocity m/s using measured fresh density and output radius)

Before pumping all hoses were washed with flowing water and a final cleaning performed by pressing a rubber sponge ball through the hoses. Then the cleaned hoses were primed with some 12 litres of cement paste before being connected to the pump and the pumping experiment started. The concrete was poured into the feeder of the pump by means of a scip and wheel barrow.

The rheological properties of the mortars were measured before (≥15 minutes after water addition) and after pumping (≥40 minutes after water addition) with a BML concentric viscometer with inner and outer diameter of 200 and 400 mm respectively. Time of start of all measurements were logged and as can be seen from Table 6, the various measurements on fresh concrete were made at quite regular intervals for the different mixes eliminating time-dependant effect or ageing of the fresh concrete considerably compared to the first two series of tests made during the development of the set-up (Jacobsen et al. 2008). Slump flow measurements were made 12 – 15 minutes and 31 – 38 minutes after water addition for the 25 and 50 Hz pumping tests, BML-viscometer measurements were made 15 – 17 and 34 – 35 minutes after water addition for the 25 and 50 Hz pumping tests. The mortars were pumped at 25 Hz 21 – 27 minutes after water addition and at 50 Hz approximately 27 to 34 minutes after water addition.

Samples of un-pumped and pumped mortar were cast in to 100 x 100 x 100 mm cubes and cured for 28 days before the compressive strengths were determined.

Table 6: Time log of measurements made during the pumping experiment (minutes after water addition)

Mix no	Before or after pumping	Slump flow/T_{50}	Air / Density	BML	Casting Cubes	Pumping	
		(min)	(min)	(min)	(min)	Hz	min
51	Before	+15	+23	+15	+25	25	27
	After	+38	+43	+35	+40	50	33
52	Before	+14	+20	+17	+22		
	After	not pumpable					
53	Before	+14	+20	+15	+20	25	24
	After	+31	+37	+38	+33	50	28
54	Before	+12	+16	+15	+16	25	21
	After	+31	+35	+34	+34	50	27
55	Before	+13	+19	+17	+22	25	31
	After	+38	+43	+34	+36	50	34

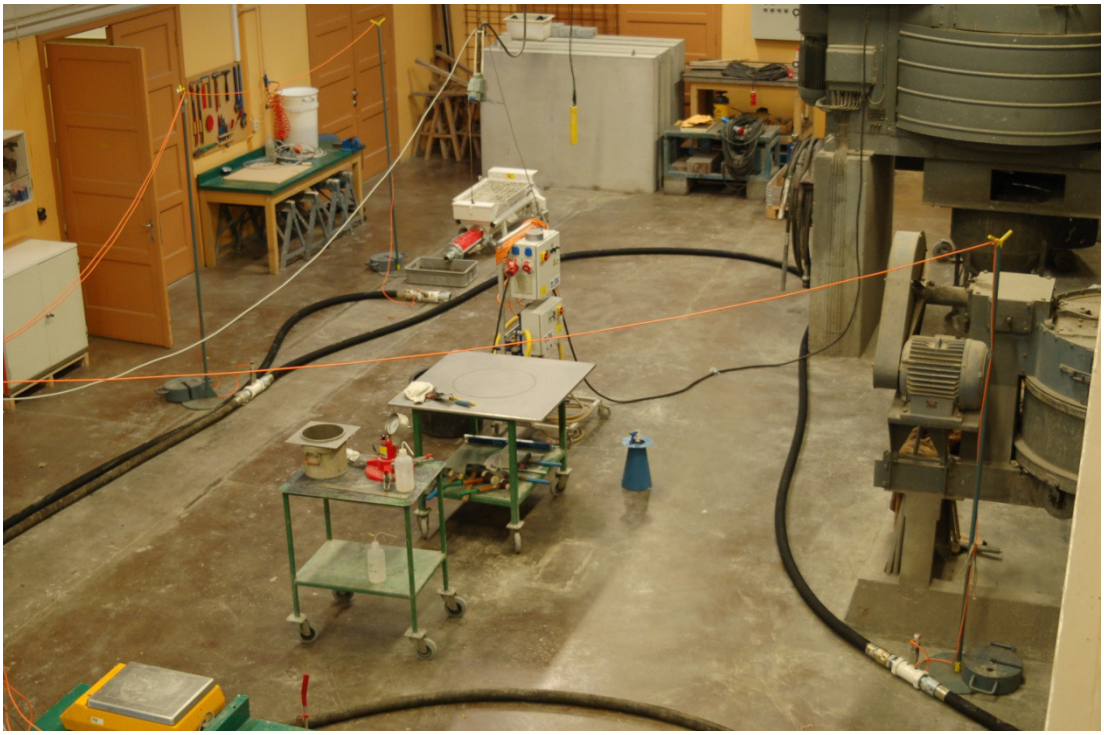

Figure 6: Pump and hose circuit with pressure sensors. The BML viscometer was located in the neighbouring room.

3.2 Results of pumping experiments

3.2.1 Rheological properties and pumpability

Rheological properties of the tested mortars are given in Table 7. Pump pressures and flow are given in Table 8.

Problems with blocking frequently occurred at the joints between the individual 13.3 m hoses and quite a lot of work was needed to disconnect the joints, shake out aggregate collected at the flow front, before reconnecting and restarting the pump. This was often repeated until a steady state flow was obtained throughout the 5 individual 13.3 m hoses that were connected. Apparently the amount of lubricating paste was not sufficient and/or tapering at joints (Ø = 45 mm) compared to the Ø 50 mm rubber hose diameter affected the flow at joints negatively, inducing blocking.

Note that Mix 52 was not pumpable when it was up-scaled to mortar. This indicates an upper limit for rheology of matrix and or mortar in order to obtain pumpable self-compacting mortars with this aggregate type and paste volume fraction. In the BML viscometer this mix had a much more plug like appearance than the other mixes that were all pumpable. Figure 7 shows snap-shots of Mix 54 from the video recordings with typical flow mode in the BML as observed by sprinkling a few grams of white filler on top of the highly flowable and pumpable concrete during viscometer test. Similar features were observed on all four pumpable mixes 51, 53, 54 and 55, showing shear-type modes of flow.

Figure 7: Shear type flow in BML with a few grams of white filler sprinkled on top to show movement

In Figure 8 the same kind of very liquid-like concrete is leaving the hose end during measurement of pressure gradient and rate of flow in the pumping test.

Figure 8: Liquid-like appearance of flow leaving hose end during pump flow measurement

A malfunction of the BML Viscometer occurred during measuring the rheological properties of mix 55 after pumping: Rotation continued at 0.5 rps, and did not follow the programmed stepwise descending. The machine was shut down and restarted before the test was started over again. This lead to some minutes extended measuring procedure, and some particle migration had possibly taken place during the uncontrolled rotation of the test bucket. In other words, the logged output is not comparable relative to the other mixes. The relatively low plastic viscosity and yield stress measured after pumping, compared to the measured values before pumping, support this assumption.

Apart from the un-pumpable mix 52, mortar viscosities measured before pumping varied within a narrow range (8.0 - 10.7 Pa·s). The yield stress before pumping had a much wider range of variation (7 - 46 Pa) and turned thus out to be the parameter with largest variation in the experiments. The work on developing a wide range of rheological properties was therefore not quite successful, probably due to choosing too narrow range of rheological properties of the pastes which were used as basis for mortars. Another possibility is the constraints of the constant water-binder ratio and constant matrix volume criterion. However, according to the study reported by Geiker et al. (2002) the relative variations from matrix to mortar should be amplified in both plastic viscosity (5 - 15x) and yield stress (50 - >100 x) when adding a constant volume of coarse aggregate. A relatively small variation in matrix rheology should, thus according to these findings, lead to a stronger variation in concrete rheology.

The rheological properties of the mortar (Table 12) can be compared with the properties of paste (Table 2) while keeping the results of Geiker et al. (2002) in mind. Table 2 shows paste yield stress values in the range 1 – 26 Pa and plastic viscosity values in the range 0.10 – 0.32 Pa·s. Yield stress and plastic viscosity measured for matrix versus mortar are given in Figure 9. Contrary to the finding of Geiker et al we find that in mortar plastic viscosity is much more affected by aggregate (in the order of 30 - 300x matrix) than yield (in the order of 2 - 3x matrix). Similar orders of magnitude were found for matrix and mortar after pumping, although with one less measurement for the un-pumpable mortar.

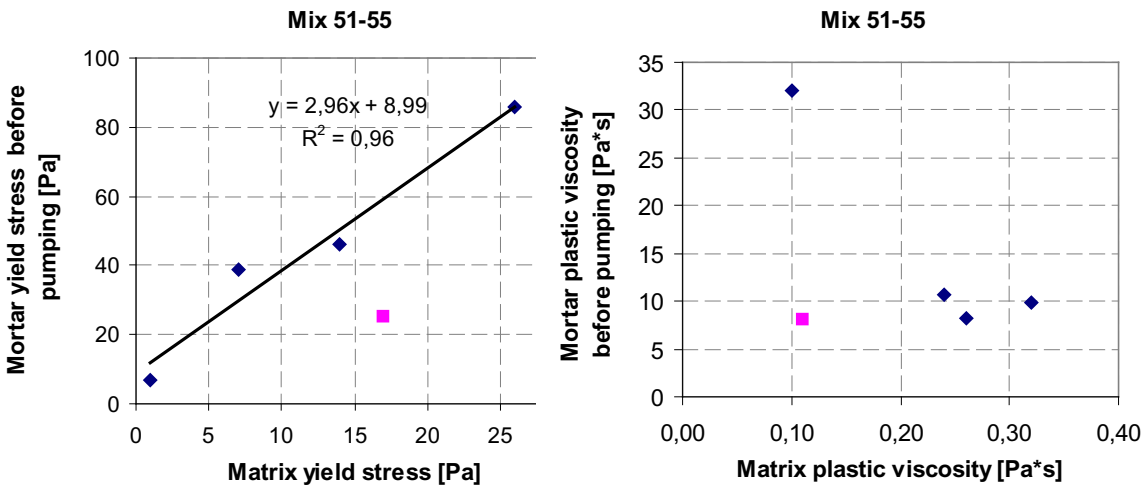

Figure 9: Yield stress and plastic viscosity of matrix and un-pumped mortar

The present results seem more reliable in terms of effect of matrix variation since we used five different paste qualities. Geiker et al. (2002) used only one paste quality with several volume fractions of aggregate. The type of aggregate was also varied within their study. They did however not perform measurements on pure paste or matrix, but merely extrapolated their model from concrete back to pure paste. When comparing paste or matrix with mortar values one should also keep in mind the effect of rheometer geometry (i.e. coaxial and parallel plate) on the measured rheological properties.

Table 7: Rheological properties of mortars used for the pumpability tests.

Mix No.	Measurement before/after pump	Yield stress (Pa)	Viscosity (Pa·s)	Slump flow (mm)	Slump (mm)	Air (%)	Density (kg/m^3)
51	Before	7	9.8	690	280	1.2	2320
	After	24	7.7	670	280	2.3	2280
52	Before	86	32.0	470	250	4.8	2240
	After	Not pumpable					
53	Before	39	10.7	580	270	1.8	2300
	After	54	8.0	500	260	1.5	2310
54	Before	46	8.2	580	270	2.0	2300
	After	88	8.4	520	265	1.6	2300
55	Before	25	8.0	670	280	1.4	2260
	After	8	3.7	760	280	1.1	2270

Table 8: Measured pump flow and pressure gradient through the hose, as well as "pumpability"

Pumping frequency (Hz)	Mix No.	dp/dx (Pa/m)	Flow (m^3/h)	Velocity (m/s)	"Normalized umpability" Flow/ (dp/dx) x10^{-4} [m^5s/kg]
25	51	15260	2.83	0,49	1.85
	52	-	-		
	53	16200	2.74	0,48	1.69
	54	13680	2.70	0,47	1.97
	55	10940	3.21	0,56	2.93
50	51	26690	5.19	0,91	1.94
	52	-	-		
	53	27180	5.18	0,90	1.91
	54	24100	5.32	0,93	2.21
	55	18830	5.71	1,00	3.03

The "Normalized pumpability" [m^5s/kg](!) calculated in the last column of table 13 is an attempt to eliminate flow variation when using dp/dx as a pumpability parameter. Note – it can only be used within one specific pump set-up. Table 13 shows that the high w/b mix 55 is best according to this simple definition. The simple "Normalized pumpability" = (G_x/(dp/dx)), which is higher the better, could be used if instrumenting a specific pump set-up with pressure sensors and flow meters to determine pumpability.

Figure 10 shows a typical measurement of flow, pressure and energy consumption observed during a pumping test. The figure illustrates that the pressures at the pump and at hose lengths of 13.3 and 26.6 m reached constant values during flow contrary to the alternating pressure/suction behaviour seen in piston-pumping (Kaplan et al. 2005). Steady-state flow was, like in earlier experiences with this pumping equipment, obtained for all pump-tests (Jacobsen et al. 2008). The pump energy also seemed to reach a practically constant value. Similar results to the ones given in this figure were obtained for all the concrete mixes at both pump frequencies used.

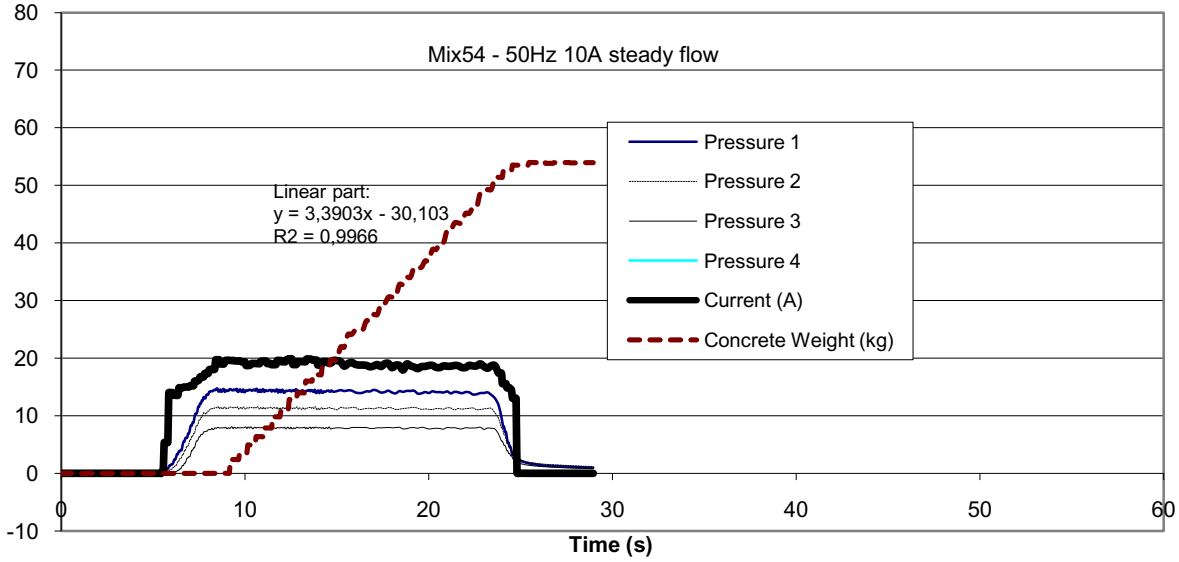

Figure 10: Typical steady-state pump flow (kg/s), pressure (bar) and current (A) measurement

The pressure profiles were basically, in accordance with previous findings (Kaplan et al. 2005), i.e. practically linear along the hose circuit as illustrated by Figure 11. Extrapolating the pressure curves linearly gives pressure values somewhat lower than the atmospheric pressure at the end of the hose , which is of course wrong. Air void content could be a reason for this effect, causing higher compression near the pump than further out along the pump line and consequently a non-linear pressure state. This is in line with three out of five mixes in Table 12 showing lower air void content after pumping.

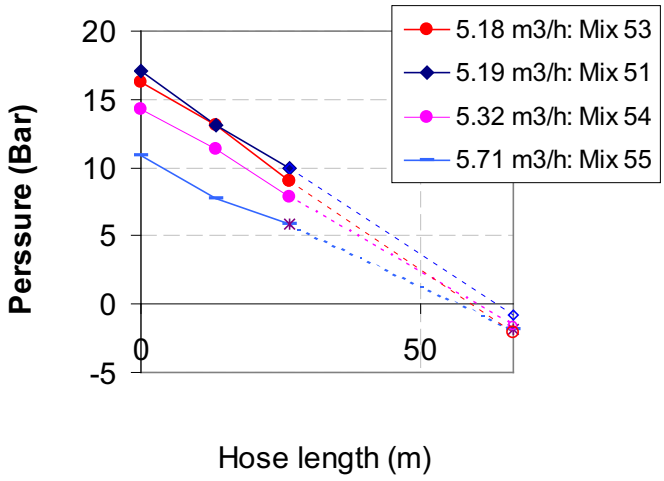

Figure 11: Pressure measured through the pipe during pumping at a frequency of 50 Hz. The stapled curves represent estimated (extrapolated) pressures.

Figure 12 gives a closer look at the measured pressure loss along the hose for mix 55 at both 25 and 50 Hz pumping. The figure illustrates that the pressure gradient is not always constant, possibly due to air voids as discussed above. The air void content was however very low, less than 2 %, for all concretes (see Table 12), but none of the other materials behaved as non-linearly as Mix 55. The non-linearity of mix 55 may be caused by air pockets that entered from the feeder. However, it is peculiar that the non-linearity seems to be stronger for the lowest pumping frequency (25 Hz). Another factor possibly affecting the

pressure is the tapering at the joints where the pressure sensors were inserted. This may have caused different pressure and flow conditions compared to in the hose. The practical problems during start of all pumping experiments with blocking at tapered joints also indicate special flow conditions there. Consequently we cannot at present state that air voids were the cause of the non-linear pressure distribution or whether this is another effect of the material. Such a material effect could for example be a better lubrication in the first part of the pumping and then reduced pressure gradient as less matrix and paste is coming from the material in the hose after some time of pressurized flow in this mix wit slightly higher w/c.

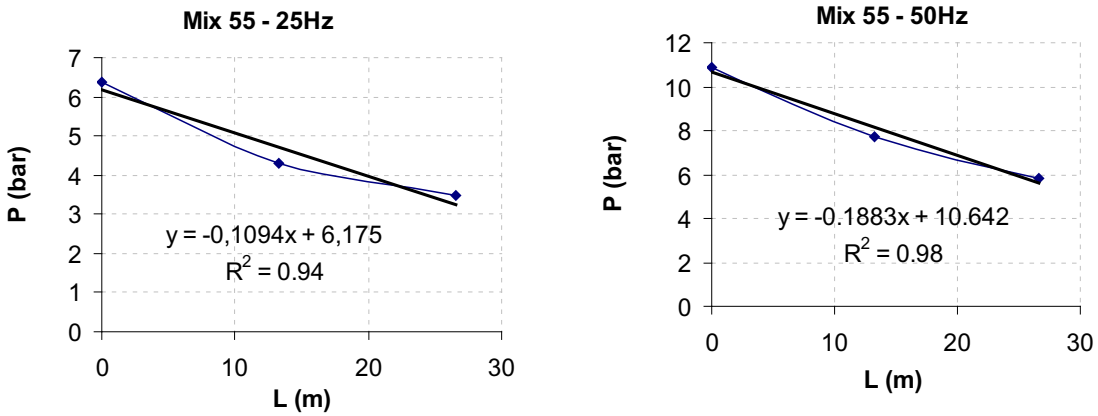

Figure 12: Close-up of pressure loss at 25 and 50 Hz of mix 55

The curves given in Figure 11 are clearly related to the paste flow curves given in Figure 4: The pumping pressures are generally reduced and the flow rate increased with increasing shear stresses of the paste.

Pressure loss measured along the hose is plotted as a function of mortar slump flow in Figure 13. It can be seen that mix 53 and 54 exhibit different pumpabilities, but identical slump flows. The slump flow data obtained in this study are thus clearly not suitable for pumpability studies. Note that slump flow is related to the yield stress. This indicates that plastic viscosity is a main parameter governing pumpability.

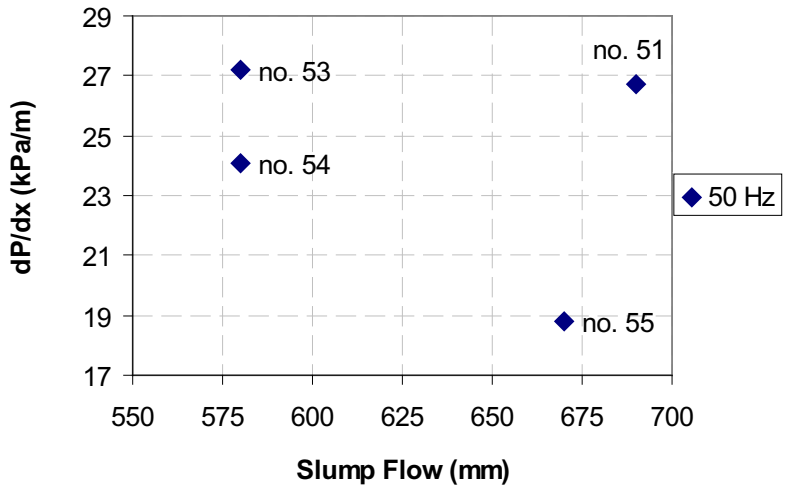

Figure 13: Pressure drop measured during pumping at 50 Hz plotted against slump flow measured before pumping. Note that mix number 52, which had a slump flow of 470 mm was unpumpable.

Figure 14 to Figure 20 illustrate the rheological properties of paste and mortar in relation to pump flow and pressure gradient. Increased viscosity of both paste (assumed to represent the slip layer) and mortar related to increased pressure drop and reduced pump flow as seen by Figure 14 and Figure 15. Note that pumping reduced the plastic viscosity of the mortar.

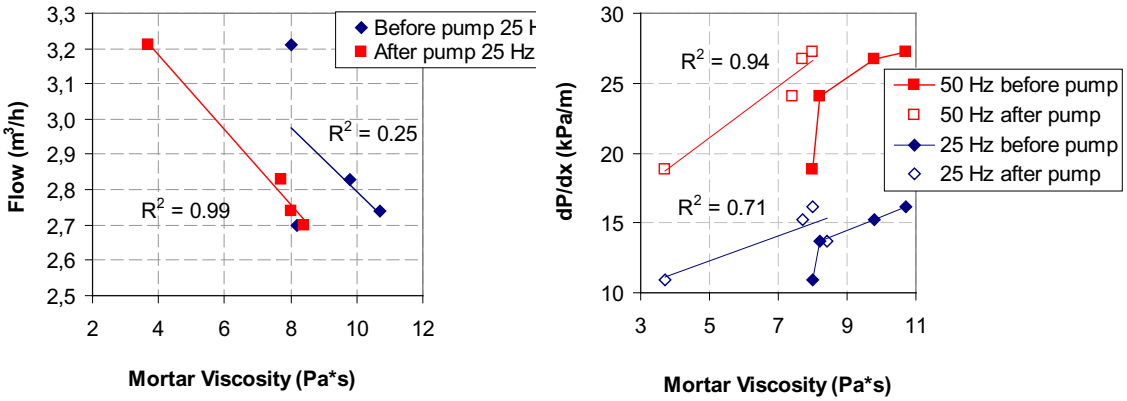

Figure 14: Mortar flow rate (left) and pressure gradient (right) as a function of mortar plastic viscosity measured before and after pumping. Regression coefficients are given for the curves obtained after pumping.

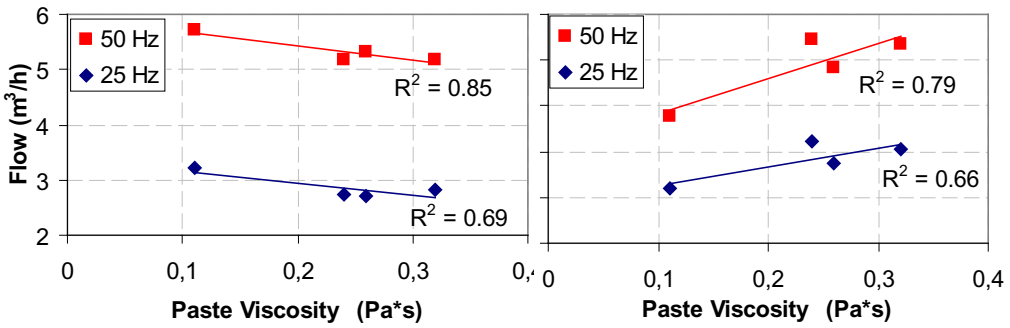

Figure 15: Mortar flow rate (left) and pressure drop (right) as a function of paste viscosity

Yield stress, gel strength and flow resistance measurements were found to follow identical trends as seen by Figure 16, Figure 17 and Figure 19. Only Bingham yield stress will therefore be discussed further in this report.

Figure 16 illustrates, surprisingly, that increased yield stress of the paste can be related to decreased pressure drop and thus increased pump flow. We find no clear explanation for this observation. It could be related to few data points. The Buckingham Reiner equation (eq.(10) predicts a larger effect of plastic viscosity than of yield on flow for the range of plastic viscosity- and yield stress values observed in this investigation. In addition there is the uncertainty of an incompressible fluid. As we have seen in Figure 11 and Figure 12 there is not a completely linear dp/dx-variation over the hose length. If the effect of pressure on volume at constant temperature, $(dV/dp)_T$, is too large then the basis for the Buckingham-Reiner equation is weakened and a continuum approach based on the complete Navier-Stokes equation must be applied (Jacobsen 2008), though not without proper experimental verification. Corresponding measurements performed on mortar were, however, not conclusive as seen by Figure 18. Mix 54 and 55 illustrate that approximately constant plastic

viscosity and reduced Bingham yield stress results in reduced pumping pressure loss, see Table 7 and 8. Mix 53 and 54 illustrates on the other hand that increased Bingham yield stress and reduced plastic viscosity results in reduced pumping pressure. The effect of reduced viscosity seems thus to dominate the effect of increased yield stress for these mixes. This finding may support previous reports of a better relationship between plastic viscosity and pumpability than between yield stress and pumpability (Jacobsen et al. 2008). The main conclusion is, however, that these parameters should not be studied independently.

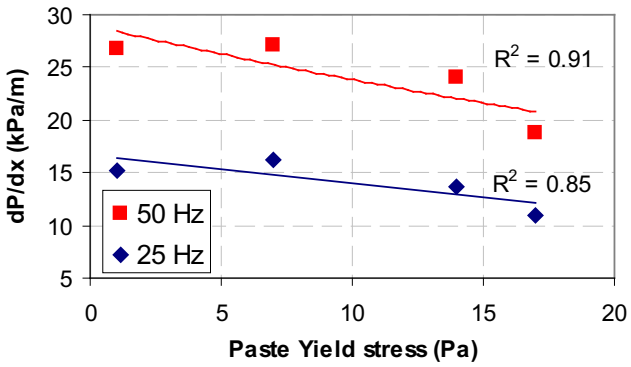

Figure 16: Mortar pressure gradient as a function of paste (Bingham) yield stress.

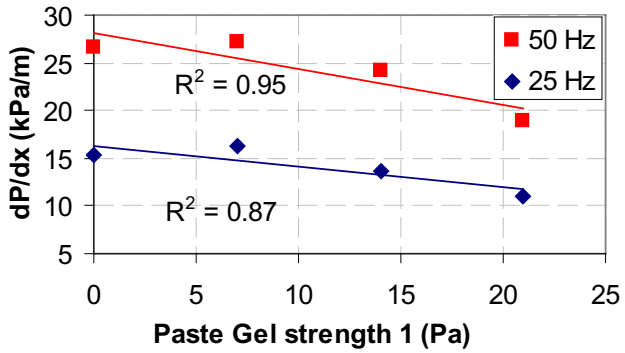

Figure 17: Mortar pressure gradient as a function of paste gel strength 1 (static yield stress).

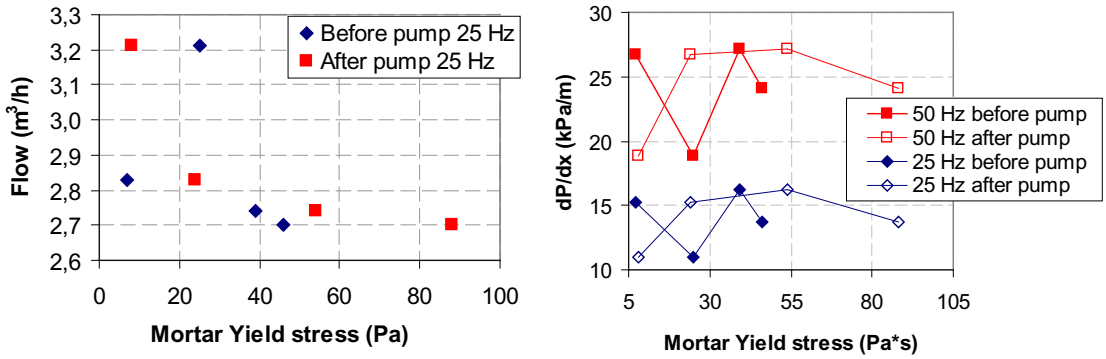

Figure 18: Mortar flow rate (left) and pressure gradient (right) as a function of paste yield stress.

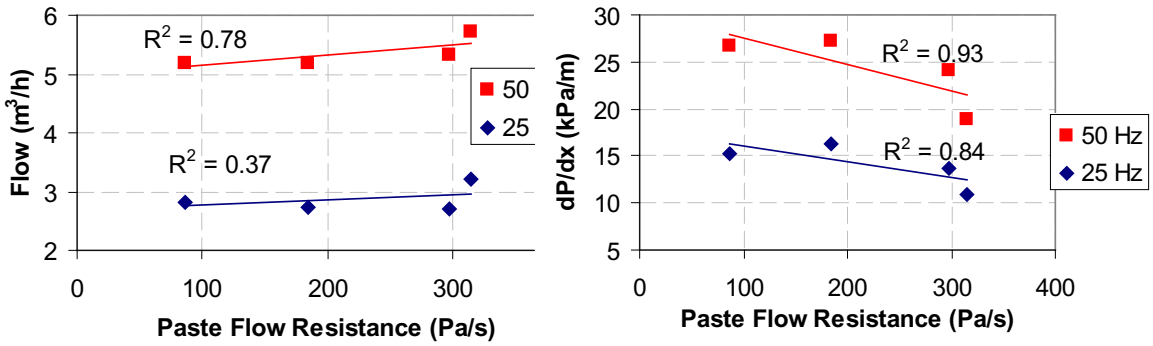

Figure 19: Mortar flow rate (left) and pressure gradient (right) as a function of paste flow resistance.

Thixotropy is defined as a gradual decrease of the viscosity under shear stress followed by a gradual recovery of structure when the stress is removed (Barnes et al. 1989). During profiled flow in pipes the shear rate is reduced with increasing distance from the wall to the centre. Breakdown of internal structure is therefore mainly occurring close to the wall while the structure will be able to rebuild as the distance from the wall increases. Note that distinguishing thixotropy from a developing slip layer can be very difficult (Barnes 1997). Thixotropic properties depend, moreover, on the rheological measurement sequence. Figure 20 indicates that the flow rate is reduced as thixotropy increases. Thixotropic properties of the paste may, thus, may be an indication of the resistance of flow within the slip layer or perhaps of gradients of rheological properties over the hose cross section during flow.

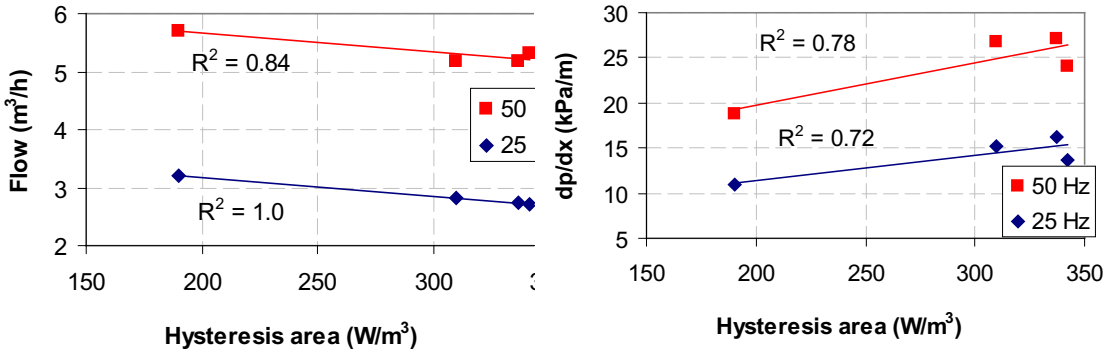

Figure 20: Mortar flow rate (left) and pressure gradient (right) as a function of paste hysteresis (thixotropy).

3.2.2 Relation between measured and calculated flow properties

The validity of the model used in this study has been checked by comparing measured and calculated pressure drop. The procedure was as follows:

- The flow rate was measured during the pumping experiments
- The theoretical flow rate was calculated by inserting measured Bingham values and pressure drop into equation (8)
- The theoretical pressure drop was found by altering the dp/dx values in equation (8) while keeping the measured Bingham values unaltered until the calculated flow rate equalled the measured value

The ratio between estimated and measured pressure losses can be found in Table 9. The predicted pressure losses are 5-7 times higher than the measured values. This indicates that one or more of the premises of the Buckingham-Reiner equation made in deriving the models used are erroneous. These premises are most probably

- homogeneous fluid
- slip-conditions at the walls

Feys (2009) found similarly from experiments pumping SCC through a piston pump and steel pipes that applying the Bingham model to Buckingham-Reiner resulted in the predicted pressure losses being 6-9 times higher than actually measured values. The ratio of predicted/measured pressure loss increased with increasing flow rate (l/s). The ratio of predicted versus measured pressure loss was reduced to 2-1 by use of the Modified Bingham equation ($\tau = \tau_y + \mu \cdot \dot{\gamma} + c \cdot \dot{\gamma}^2$, where c is a second order fitting parameter).

Thus, these findings are in line with Kaplan (2001) who reported that there is a contribution of slippage to the velocity (i.e. that a lubrication layer is formed by the wall). Kaplan estimated that the thickness of the slippage layer corresponds to the maximal distance the coarse aggregate can move to reach maximal packing in the centre of the pipe. It is correspondingly reasonable to assume that the rheological properties of the concrete are not constant, but vary along the cross section of the tube (i.e. decreasing viscosity and yield stress from the centre of the tube (plug) to the wall). A main challenge will thus be to find a method to measure and/or calculate velocity and thickness of the slippage layer. As already mentioned we will pursue this and some slip –layer calculations have been made in the next sub-section.

Table 9: Estimated and measured pressure loss. Calculations are based on Bingham parameters measured on concrete before pumping.

Pumping frequency (Hz)	Mix No.	Estimated dp/dx (Pa/m)	Measured dp/dx (Pa/m)	$\frac{(dp/dx)^{estimated}}{(dp/dx)^{measured}}$
25	51	77500	15260	5.1
	52	-	-	-
	53	85500	16200	5.3
	54	66600	13680	4.9
	55	73850	10940	6.8
50	51	141300	26690	5.3
	52	-	-	-
	53	157600	27180	5.8
	54	125900	24100	5.2
	55	129100	18830	6.9

Plug radii calculated by aid of measured and estimated pressure losses are given in Table 15. A flow profile calculated by aid of measured pressure loss and Bingham parameters is represented by Figure 21. Velocity profiles of the other mixes are given in Appendix A2. Table 15 shows that the plug radius decreases with increasing pumping frequency as expected. Mix 51 has a marked smaller plug than mix 53-55. The latter mixes tend, moreover, to have similar flow profiles. Note that plug radii calculated by aid of estimated pressure drop, and thus an assumption of no slip layer, are smaller than if measured pressure drop values are used.

From visual observations of the mortar flow pattern during testing in the concentric BML viscometer, observations of a liquid like flow behaviour at the output of the pump hose, and observations made separately with gravitational flow experiments (Jacobsen et al. 2009), the kind of flow profile shown in Figure 21 seems probable. However, this does not explain the reason for the low flow predicted by the Buckingham-Reiner equation. Table 14 shows that the estimated pressure required to reach our flow is in the order 5 – 8 times what we measure. The existence of a layer close to the pipe wall with rheological properties giving higher flow is possible as already discussed. This could also be some kind of gradient of rheological properties over the pipe cross section (and length?). This could again be due to factors like segregation of aggregate, squeezing out of matrix and water towards wall, and also variation of shear rate and probably also effects of thixotropy due to differences in stiffening over the cross section during flow. Whatever reason there are a number of complicating factors that may contribute to the peculiar fact that we are not able to predict this relatively simple flow case with constant pressure drop and flow velocity through a cylindrical pipe.

Table 10: Plug radius calculated with measured and estimated values of dp/dx. The calculations are based on Bingham parameters measured on concrete before pumping.

Pumping frequency (Hz)	**Mix No.**	**Plug radius, R_p, (mm) calculated from measured dp/dx**	**Plug radius, R_p, (mm) calculated from estimated dp/dx**
25	51	0.9	0.2
	52	--	-
	53	4.8	0.9
	54	6.7	1.4
	55	4.6	0.7
50	51	0.5	0.1
	52	-	-
	53	2.9	0.5
	54	3.8	0.7
	55	2.7	0.4

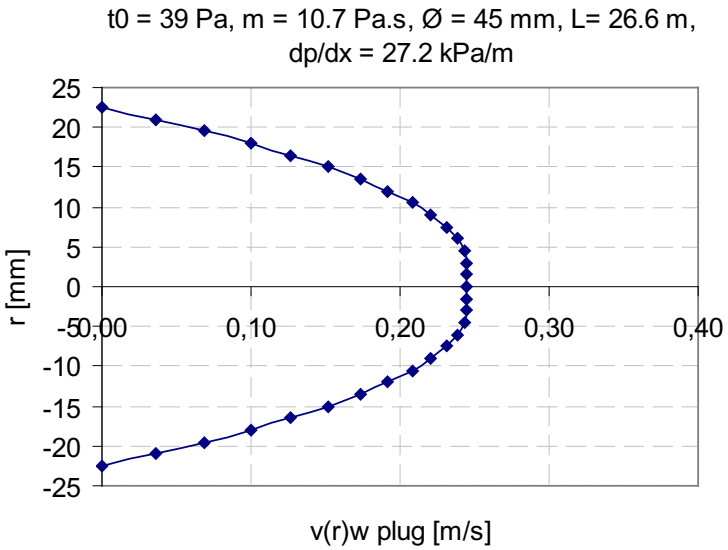

Figure 21: Velocity profile calculated with measured values of pressure drop, plastic viscosity and yield stress as a function of tube radius of pumped concrete, Mix 53.

3.2.3 Slip layer properties and estimation of thickness

We have made an effort to improve the prediction of pumpability from rheological properties. This is done by using all our measurements and assuming slip at the wall and altered rheological properties of the slip layer compared to the mortar. We introduce slip into the plug flow equation, eq. (8):

$$v(r) = [\frac{1}{4\mu} \cdot \frac{dp}{dx}(a^2 - r^2) - \frac{\tau_{y,mortar}}{\mu}(a - r)], r \geq R_p$$

$$v(r) = v(R_p), r < R_p$$

Without slip but with plug radius $R_0 = 2\tau_{y,mortar} / (dp/dx)$ v(r) is integrated to give total flow $G_x = v_x \pi a^2$ on the usual form shown in eq. (10).

The slip layer thickness $(a - R_p)$ can then be estimated from measurements of flow and pressure gradient in pumping tests of concrete, and measurements of assumed slip layer rheology in parallel plate viscometer tests on matrix of the same composition as in the concrete. We then solve iteratively (in Excel) for the slip layer thickness $(a - R_0)$ by assuming $R_p \neq 2\tau_{y,mortar} / (dp/dx)$ and requiring that the integration of equation (8) as shown in eq.(12), which has a discontinuous derivative as $r = R_p$, equals total measured flow:

$$\int_0^a v(r)dr = v_{x,measured} \tag{12}$$

where $v_{x,measured}$ is measured flow in the pumping test, and using

$\frac{dp}{dx}$: measured in the pumping test

τ_y, μ: measured in parallel plate viscometer on matrix assumed to represent the slip layer (Vikan et al (2009)).

The procedure for estimating thickness of slip layer is based on stepwise integration of eq.(12) in 0.5 mm layers or radial segments in Excel. An iterative procedure briefly introduced in [Jacobsen et al 2008] is used fitting the flow of a plug surrounded by a material between plug and wall that has unknown rheology. The measurements from instrumented pump test give real flow and real dp/dx, and viscosimetry of mortar and paste can be taken as maximum and minimum possible viscosity of slip layer.

The yield stress of matrix is quite high compared to mortar, as already discussed based on comparison with earlier research, but is consistent from matrix measurements when performing both the gel-strength test [Vikan 2005] and using Bingham curve fitting. However, with the actual slip model the yield of the slip layer, as for yield of the concrete, has little effect on flow calculated with Buckingham Reiner within normal variation of mortar. This is easily verified by running a series of calculations with in excel. Plastic viscosity, including slip layer plastic viscosity, has however a large effect on flow. Therefore yield is kept constant.

We start with the plug radius calculated straightforward from dp/dx and yield in mortar for actual pumping experiments, as shown in the previous subsection. This then gives a flow which is too low compared to measured flow as already discussed.

Then we adapt the viscosity of the slip layer so that measured flow fits calculated plug flow at measured dp/dx. The thickness and viscosity of the slip layer are both reduced in a stepwise manner, while keeping flow constant and equal to measured flow for each step. That is, either the viscosity or the thickness is chosen and then the other property is adapted to right flow for actual pressure gradient. This is repeated until plastic viscosity measured on matrix in parallel plate viscometer is reached. Due to the low sensitivity of calculated flow to yield stress variation, the measured yield stress value is kept constant as discussed. However, we remind that the plug can only exist due to the yield stress.

Examples of plots of plug flow profiles according to this method are shown in Figure 22-Figure 1. They show three different flow profiles for mix 54 pumped at 50 Hz. All calculations are carried out with the measured total flow of 0.93 m/s and measured pressure gradient of 24100 Pa/m for the actual pumping experiment.

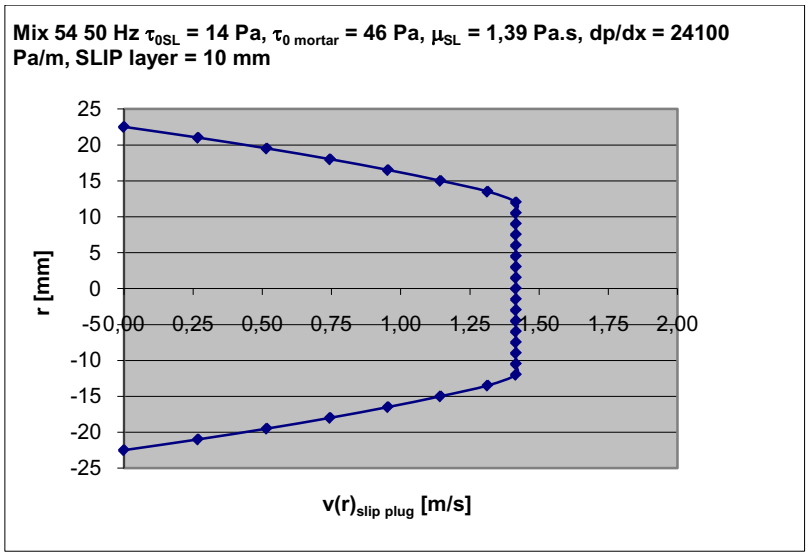

Figure 22: Mix 54 pumped at 50 Hz with 0.93 m/s output with 10 mm slip layer, plastic viscosity of slip layer estimated at 1.39 Pa·s

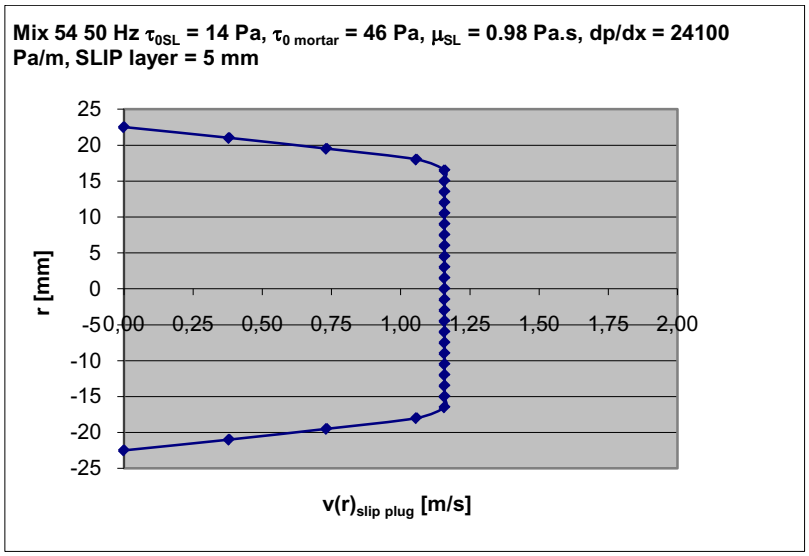

Figure 23: Mix 54 pumped at 50 Hz with 0.93m m/s output with 5 mm slip layer, plastic viscosity of slip layer estimated at 0.98 Pa·s

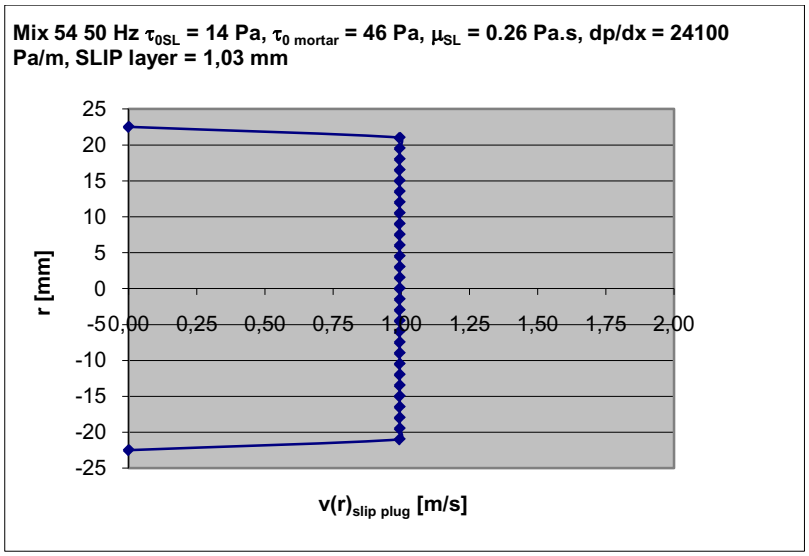

Figure 24: Mix 54 pumped at 50 Hz with 0.93m m/s output with 1 mm slip layer, plastic viscosity of slip layer as measured in matrix = 0.26 Pa˙s

Figure 25 shows how the slip layer thickness reduces at reducing plastic viscosity at the measured flow and pressure gradient, starting with the plug radius calculated with the Bingham parameters of the pumped mortar measured with the BML viscometer and reducing as the slip layer viscosity reduces to the measured value of the matrix.

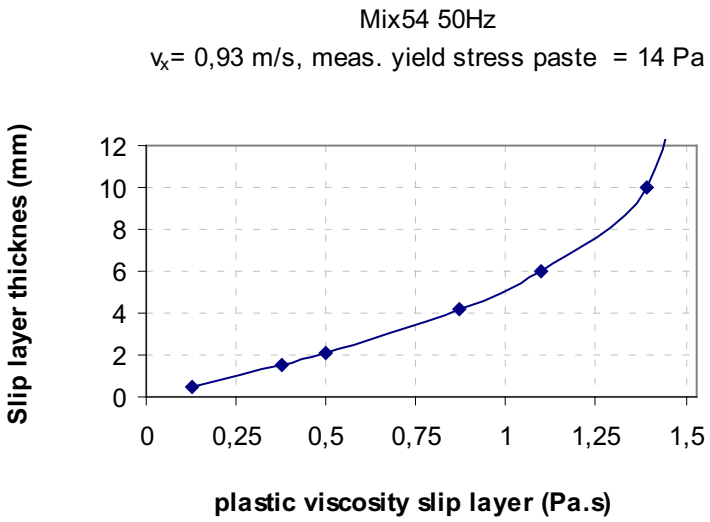

Figure 25: Slip layer plastic viscosity vs thickness at constant flow = 0.93 m/s for mix 55 pumped at 50 Hz

In Figure 24 the rheological properties of the slip layer equals that measured with parallel plate viscometer on the matrix for the actual mix. The feature of the plug appears somewhat different from the shape of the flow profiles visualized and observed in [Jacobsen at el 2009]. However, in that experiment the flow velocity was only 0.3 m/s in the rubber pipe of the equivalent mix, the pressure was very low and the flow length was only a bit more than 1 meter contrary to almost 70 meters in the pumping experiment. Furthermore, the visual appearance of the output from the hose end of the actually pumped material, which was video filmed, was definitely not a plug but a very liquid-like concrete as it left the hose. At an average flow rate of 0.93 m/s the concrete spends more than a minute in the almost 70

metres of hose and possibly there is time for some kind of stiffening for the central part of the concrete with the least shear action.

Since there is a steady state flow with constant pressure drop this kind of in-hose stiffening seems realistic in this experiment. However, this does not explain similar discrepancies between the Buckingham Reiner equation and observed flow in piston pumping with the alternating pressure/suction behaviour and probably more unfavourable conditions for plug formation due to in-line stiffening. Possibly the steel pipes in normal concrete piston pumping like in the studies by Rössig (1974), Brown and Bamforth (1977), Hansen (1988), Hu and deLarrard (1996), Kaplan (2001) and Feys (2009) provide higher flow near the pipe wall. This was indicated by more plug shaped flow profiles in steel compared to in rubber pipes in [Jacobsen et al 2009]. Another viewpoint that can be taken is that the same kind of fundamental problem compared to the ideal plug flow exists in both screw- and piston pumping with the kind of central coarse aggregate segregation proposed by Kaplan (2001). However, this "central coarse aggregate segregation" should then rely on rotation of aggregate particles and more radial movement than we would expect with just a thin slip layer. Haist and Mueller (2005) observed this slip layer, whereas stiffening in the hose would reduce movement and rotation of particles in the core. We cannot conclude on this here. In Table 11 we have tabulated the slip layer thickness calculated as explained above for all 8 pumping tests conducted on 4 materials each at 2 pump frequencies.

Table 11: Estimated slip layer thickness [mm] and slip layer viscosities

Mix number	Frequency (Hz)	Slip layer thickness at measured plastic viscosity (mm)	Slip layer viscosity (Pa·s/m)
51	25	1.00	320
51	50	1.06	302
53	25	0.85	282
53	50	0.79	304
54	25	0.96	271
54	50	1.03	252
55	25	0.63	175
55	50	0.61	180

Table 11 shows that all mixes have remarkably equal thicknesses of the slip layer, even at the two different pump frequencies. Mix 55 with somewhat higher w/b has somewhat lower thickness in accordance with its low plastic viscosity. The calculated thicknesses are equal at the two pump frequencies, as would be expected from the approximate proportionality of pressure and flow and assumed linearity of the rheology in the narrow slip layer between the plug and the pipe wall from the Bingham model. It seems thus that the matrix can lubricate a very thin slip layer. However, water could lubricate an even thinner slip layer. This should be further investigated.

The specific plastic viscosities of the slip layer in Table 11 are of the same magnitudes as the lower range measured by (Kaplan (2001) pp.144-145) in his tribometre. This too indicates that slip layers are very thin during pumping compared to in tribometre measurements made at atmospheric pressure. The viscometer measurements of our study are performed at atmospheric pressure. However, our conversion to slip zone plastic viscosity is based on the iterative calculation using both measured pressure and measured flow in the pressurized pumping experiment, as well as the matrix properties measured in the parallel plate viscometer. We believe this makes the slip layer estimate closer to reality.

From the flow profiles shown in Figure 22 – Figure 24 we can also estimate the average rate of shear in the slip zone from the basic relation:

$$\frac{dv(r)}{dr} = \dot{\gamma} \tag{13}$$

Which for the estimated slip zones of our experiments can be approximated by the relation:

$$\frac{\Delta v_{plug}}{a - R_p} \approx \dot{\gamma} \tag{14}$$

Where the plug velocity Δv_{plug} is found in Figure 22 – Figure 24. Table 12 shows the estimated rates of shear of Mix 55 pumped at 50 Hz.

Table 12: Estimated rate of shear in slip zones of Mix 55 at 50 Hz

$\geq \Delta v_{plug}$ (m/s)	a-R_p (m)	$\dot{\gamma}$ (1/s)
1,4	0,01	140
1,15	0,005	230
1	0,001	1000

From Table 12 we see that the rate of shear will be very high for a slip layer with the same rheological properties as the matrix. But even for the thicker slip zones the average rate of shear is quite high compared to what is used in the parallel plate viscometer (=max 100 s^{-1}, see appendix). In future tests the viscometer should be run up to 1000 s^{-1} to check whether the rheological properties of the actual matrix can be described by the very simple Bingham model over the whole range of shear. We have seen both shear thinning and hear thickening behaviour during the development of the present materials. Consequently, the Bingham parameters might not hold for such high rates of shear and the above calculation might be jeopardized. Investigations of such high shear rates were made in the same instrument (Physica) by Koetze et al (2008) showing strong non-linearity much better described by power laws than by Bingham for some non-cementitious materials.

3.2.4 Compressive strength

Compressive strengths measured on samples cast before and after pumping are given in Table 13. The data illustrate that the pumping did not have a negative effect on the strength of the mortar, and thus indicate very good pumpability with respect to strength. We also see the low strength of Mix 55 in accordance with its high w/b, and the high strength of Mix 53 and 54 in accordance with the use of silica fume.

Table 13: Compressive strength measured on samples cast before and after pumping.

Sample	Cast	Compressive strength (MPa)
Mix 51	Before pumping	55.0
Mix 51	After pumping	53.5
Mix 52	Before pumping (not pumpable)	47.8
Mix 53	Before pumping	61.3
Mix 53	After pumping	63.8
Mix 54	Before pumping	59.4
Mix 54	After pumping	60.0
Mix 55	Before pumping	37.1
Mix 55	After pumping	40.1

3.2.5 Limitations of the study

The results obtained from this study have several limitations:

1. The relatively low number of data points due to the laborious nature of this kind of research
2. Choice of rheological model. The Bingham model was used throughout the study. Shear thinning was observed for some mixes. The Herschel Bulkley model was, however, not used due to its unrealistic (negative) yield stress results.
3. The different flow conditions through a screw and a piston pump as well as the different flow conditions of self-compacting mortar and traditional concrete should be kept in mind. A mortar or concrete will be transported as a plug through the hose if the yield stress in the mortar or concrete is high enough while the shear stress in the slip layer has surpassed the yield of the paste.
4. The possibility of increasing back-flow in the screw pump (steel screw in rubber stator) as pressure increases limiting the driving pressure.
5. There can be effects on rheology of high pressure in the pipeline as opposed to the atmospheric pressure in the viscometers.

4 Conclusions

Slump flow is not suitable for differentiating pumpability. Interpretation of rheological data was, moreover, complicated since the measured values of plastic viscosity and yield stress were altered simultaneously from mix to mix.

The data imply that both yield stress and plastic viscosity govern pumpability. Increased plastic viscosity of mortar and paste was found to correlate with decreased mortar pumpability. No clear trends could be found for mortar yield stress. Increased paste yield stress was, however surprisingly, related to increased pumpability. The plastic viscosity seemed still to dominate yield stress when the two factors varied simultaneously within the given workability range. These parameters should therefore not be studied independently.

Measured values for flow rate, G_x, plastic viscosity and yield stress have been used to estimate the theoretical pressure drop in order to check the validity of the Bukingham-Reiner and Bingham equations used in this study. The predicted pressure losses are 5-7 times higher than the measured values. This indicates that one or more of the premises of the Buckingham-Reiner equation made in deriving the models used are erroneous. These premises are homogeneous fluid and no slippage at the walls.

Increased hysteresis area calculated from the paste measurements correlated very well with reduced pump flow indicating a relation to the rheology of the slip layer.

The existence of a plug was based on the observation of yield stress both in the BML- and in the parallel plate viscometer as well as visualized flow profiles in a separate study. The yield stress-ratio matrix/mortar was surprisingly high compared to the plastic viscosity-ratio matrix/mortar. Separate gel-strength tests correlated well to the matrix yield stress for the 5 final mixes studied. The Buckingham Reiner equation was used in an iterative procedure applying measured flow and slip zone plastic viscosity approaching measured values in the parallel plate viscometer. This resulted in slip zone thickness in the order of 0.6 – 1 mm. The results were not very sensitive to variations in yield stress, whereas plastic viscosity had a major effect as shown in plots of slip zone viscosity vs. slip zone thickness. For measured matrix viscosity, the calculated specific viscosities (Pa·s/m) were all similar to the lowest values reported by Kaplan (2001). We are of the opinion that the combination of instrumented steady state pumping, parallel plate viscometer and visualized boundary flow rate give better prediction of slip layers than the tribometre of Kaplan (2001). Finally we attribute the slip layer existence to its high shear rate compared to that of the concrete in the core. The latter may act as a plug due to stiffening and thixotropic behaviour during more than one minute in the steady state pump-flow. The average rates of shear in the slip zone were estimated as high as 1000 [s^{-1}]. This is much higher than those used in the parallel plate viscometer (100 [s^{-1}]).

These findings are in line with former studies; there is a contribution of slippage to the velocity (i.e. that a lubrication layer is formed by the wall). It is, correspondingly, reasonable to assume that the rheological properties of the concrete are not constant, but vary along the cross section of the tube (i.e. decreasing viscosity and yield stress from the centre of the tube (plug) to the wall). A main challenge is to determine the actual flow conditions in the pipe under pressurized flow.

We would finally like to emphasize the indicative nature of our findings due to the relatively low number of data points. A weakness of functional relationships between acting shear rate and resulting yield stress, modelled by for instance Bingham, Herschel-Bulkley etc, is that certain models may fit better to certain types of materials. In addition, pressure effects in the pipeline might result in other rheological properties than those measured at atmospheric pressure in the viscometer.

5 Recommended further research

More work is needed in order to identify which material parameters govern pumpability of concrete. These are fundamental parameters which we expect will influence several types of flow of concrete such as pumping, form-filling and flow against solid surfaces. The material behaviour may depend on pressure which complicates the characterization of flow in pipes. Pipe flow is, however, a simple and well defined flow case compared to the filling of a formwork with reinforcement.

The results reported in this study indicate, in accordance with other authors, the occurrence of a slip-layer during pumping. Further experiments should therefore try to verify the existence of a slip layer in some way. This could for example be by flow visualization or use of tribomter.

Visualization of the slip layer and flow profile could be achieved by developing an ultrasound based in-line viscometer. A prototype can be developed in cooperation with world-leading technologists on this field, Johan Wiklund and Mads Stadig at SIK (Göteborg). Especially sensor technology and signal treatment needs to be developed. The result will be a method that is easy to use and independent of the operator. The prototype is stipulated to need approximately 1 mill NOK. These costs are assigned to equipment needed for the prototype, namely sensors (SEK 40'), measurement cell (SEK 50'), pulse/receiver (SEK 200 – 400') and development of software (SEK 450'.)

More experimental data including paste viscosity, and flow resistance measured as the area under the rheological flow curve is needed in order to map material properties governing pumpability and obtain more advanced modelling. Thixotropy is of course a complicating factor which is not described by any of the flow models we have used so far (Bingham, Herschel Bulkley, Carreau). This is probably of importance since the slip layer estimates indicate that most of the concrete in the pipe flows like some sort of stiffened plug.

Additional mixes with workabilities complimentary to the ones already performed are needed in order to clarify the findings given in this report. Four new mixes are suggested in Table 14.

Future parallel plate viscometer tests in studies of this kind could be carried out to 1000 [s^{-1}].

Table 14: Suggested new mortar mixes (blue) and already pumped mixes (white).

Mix No.	w/b	Silica fume (%)	Filler (%)	Superplasticizer (%)	Stabilizer (%)
1 - ref	0.50	0.0	0.0	0.0	0
51	0.50	0.0	0.0	1.0	0
56	0.50	2.5	0	0	0
57	0.50	2.5	0.0	1.0	0
52	0.50	2.5	0.0	2.0	1
55	0.56	2.5	0.0	2.0	1
3	0.50	5.0	0.0	1.0	0
54	0.50	5.0	0.0	0.8	0
53	0.50	5.0	12.5	1.2	0

It is moreover interesting to study the influence of pump type on this kind of study: It seems like the viscosity is the dominating property regarding pump ability for the rotor pump, while for a piston pump, with off and on pressure cycles, the yield stress is the main governing parameter. The influence of pump type, such as piston and screw pump, on the correlations between rheological properties of pumped materials and pumpability should therefore be

studied. Larger pumps will, moreover, enable pumping of concretes with larger aggregate size than 8 mm as used in this study. It is accordingly recommended to study the influence of aggregate size on pumpability.

In spite of the improved flow calculation we think that there is much more work to be done. Understanding flow conditions in more complex flow cases than in the steady state flow through a straight pipe seems difficult at present. Furthermore we have not been able to verify the actual flow conditions inside the pipe during pressurized pumping with our screw pump. As already discussed, the outflow material certainly gave no impression of a plug. In addition to understanding the clearly more complex case with piston pumps and the slip conditions of steel pipes, we also need to understand how the local flow conditions near the surface affect compaction and presence of voids as well as how the passing between narrow passages during form filling affects flow properties.

An extensive preliminary study has been performed on the free flow profile (not pumped, but flowing under due to gravitational forces) of coloured mortars (Jacobsen et al. 2009). The results have shown that the type of tube material in which the mortar is flowing is of importance to the flow profiles. Full-scale pumping experiments with different tube materials (for instance steel) could therefore be conducted.

Possibly high speed camera filming of the concrete as it leaves the hose end can disclose any sign of structure breaking up, whereas the kind of matrix-rich layer measured by Haist and Mueller (2005) could disclose an in-line slip layer.

Another possible topic of research is the measurement or observation of slip layer thickness in a similar way as mentioned above during form filling.

Surfaces (hose, formwork) should at least be quantified by their roughness. If the slip layer is made up of only water (with viscosity = 0.001 Pa·s = 1/100 – 1/320 of the equivalent Bingham viscosity value of the matrix) then the slip layer consists of a very thin layer of water in accordance with figure D. The thin water layer should in that case be thick enough to smoothen any effect of surface roughness of the solid surface the concrete is flowing along. For the pipe materials we are considering (rubber, steel) the roughness is probably in the order of the maximum size of cement grains according to the SEM – pictures in Jacobsen et al (2009), i.e less than 0.1 mm.

6 Acknowledgement

Thanks to Mårten Ekelin, Bruno Jensen, Jon Håvard Mork (maxit Saint Gobain Weber, Malmö, Sweden), Louis Samuel Bolduc (Laval University, Canada), Siaw Foon Lee, Ove and Gøran Loraas, Andreas Gurk NTNU for help with organising and carrying out the experiments.

References

ACI Comm. 304 (1998) Placing concrete by pumping methods, ACI 304.2R-96, 2nd Print 25p.

Barnes, H. A., and Walters, K., "The yield stress myth?", Rheol Acta 24 (1985) 323-326

Barnes H.A, J.F. Hutton, K. Walters, An Introduction to Rheology, Elsevier Science, Amsterdam, 1989

Barnes H.A., Thixotropy – a review, J. Non-Newtonian Fluid Mech., 70 (1997) 1-33

Billberg P. (2006) Form Pressure generated by Self-Compacting Concrete – Influence of Thixotropy and Structural Behaviour at Rest, Doctoral Thesis, KTH Stockholm ISBN 91-7178-464-0 (2006) 91 p. + 5 papers

Browne Roger.D, Bamforth Phillip B. (1977) Tests to establish concrete pumpability, ACI Journal May 1977, 193-203

Feys D., Interactions between Rheological Properties and Pumping of self-Compacting Concreye, PhD Thesis Ghent University, 2009, ISBN 978-90-8578-277-3

Feys D., Verhoeven R., De Schutter G., Full scale pumping tests on SCC: Test description and results, in Proceedings of SCC 2008 Chicago, Session A4

Geiker M., Brandl M., Thrane L., Nielsen L., On the Effect of Coarse Aggregate Fraction and Shape on the Rheological Properties of Self-Compacting Concrete, *Cem. Conc. Agg,.* 24(1) (2002) 3-6

Haist M., Müller H.S.(2005) Optimization of the pumpability of self-compacting Light Weight Concrete, Proc SCC 2005 ACBM, NWU, Evanston, 6 p.

Hansen J.K.B., (1988) Characterisation of concrete pumpability using the two-point apparatus, High Performance Concrete materials Development report 3.2, SINTEF Report STF 65 F89046, Norway, p. 45

Hu C., De Larrard F., Sedran T. (1996) A new rheometer for high performance concrete, 4th Int Symp on High Strength/High performance concrete, Presses de LCPC, 179-186

Kaplan D., de Larrard F., Sedran T., Design of Concrete Pumping Circuit, *ACI Materials Journal,* March-April (2005) 110-117

Kaplan D.(2001) Pompage des bétons, Thèse de doctorat ENPC/ LCPC, ISBN 2-7208-2010-5, Paris, 228 p.

Jacobsen S., Haugan L., Hammer T.A., Kalogiannidis E., Flow conditions of fresh mortar and concrete in different pipes, *Cem. Concr. Res.*, **39** (2009,) 997-1006

Jacobsen S., Mork J. H., Lee S.F., Haugan L., Pumping of concrete and mortar – State of the art, COIN Project Report no. 5 2008, ISBN 978-82-536-1069-6

Jolin M., Chapdelaine F., Burns D., Gagnon F., Baupré D.(2006) Pumping concrete; a fundamental and practical approach, presentation Shotcrete for underground support X, Sept.12-16 (2006) 9 p.

Koetze R. et al (2008) Rheological characterization of highly concentrated minera suspensions using ultrasound velocity profiling with combined pressure difference method, Appl.Rheol. 18, 62114-1-62114-10

Rössig M.(1974) Fördern von Frischbeton, insbesondere von Leichtbeton, durch Rohrleitungen, Dr.diss, RWTH, Westdeutscher Verlag, ISBN 3-531-02456-6, 132 p. + 92 p. fig/tab

Sakuta M., Kasanu I., Yamane S., Sakamoto A. (1989), Pumpability of fresh concrete, Takenaka Technical Research laboratory, Tokyo, pp. 125-133

Smeplass S., Mørtsell E., "The Particle Matrix Model applied on SCC", In Proceedings of the Second International symposium on Self-Compacting Concrete, 23-25 October 2001, Tokyo, Japan, 267-276

Tattersall G.H., Banfill P.F.G.(1983) The Rheology of Fresh Concrete, Pitman Books Ltd., London, 356 p.

Yahia, A. and Khayat, K.H., "Analytical models for estimating yield stress of high-performance pseudoplastic grout", *Cem. Concr. Res.* **31** (2001) 731-738

Vikan, H., Justnes, H., Winnefeld F., Figi, R., "Correlating cement characteristics with rheology of paste" *Cement and Concrete Research*, **Vol 37 (11)** (2007) pp. 1502-1511

Vikan, H., "Rheology and reactivity of cementitious binders with plasticizers", Doctoral Theses at NTNU 2005:189, Also available at http://www.diva-portal.org/ntnu/theses/abstract.xsql?dbid=689

Vikan H., Jacobsen S., Haugan L., Rheology and pumpability of mortar, Proceedings of the 3rd International RILEM Symposium on Rheology of Cement Suspensions such as Fresh Concrete, 2009 Reykjavik Iceland, PRO 68, ISBN 978-2-35158-091-2 (2009) pp. 88-96

Wallevik J.E. (2003) Rheology of particle suspensions Fresh Concrete, Mortar and Cement paste with various types of lignolsulfonates, PhD 2003:18 Dept of Structural Eng, NTNU 397 p.

Wiklund J.(2007) Ultrasound Doppler Based In-Line Rheometry, development, validation and application, Doctoral thesis Lund University ISBN 978-91-628-7025-6, 81 p. + 5 papers

APPENDIX A1– Preliminary recipe devolpment

Development of pastes

These pilot- or pre-mixes were made and studied in order to obtain pastes with as different rheological properties as possible. The paste recipes were used as basis for development of mortars. Mix 1-8 were pilot- or pre-mixes aiming at obtaining pastes with as different rheological properties as possible. That is, typically one paste with high viscosity and high yield stress, one paste with high viscosity and low yield stress, one paste with low viscosity and low yield stress and last one paste with low viscosity and high yield stress. It was assumed that these variations would then be similar in mortar.

Materials and recipes

The following materials were used for the paste experiments:

- Portland cement of type CEM II/A-V (containing 20 % low lime fly ash)
- Silica fume (Elkem Microsilica Grade 940)
- Filler with a particle size smaller than 0.125 mm, retrieved from the granitic sand by sieving
- Superplasticizer (Glenium 151 with 15±1 % dry material)
- Viscosity modifying stabilizer (Sika Stabilizer 4R with ca. 5 % dry material)
- Black concrete colouring agent used in other parts of the project to study concrete flow profiles

All paste recipes are given in Table 1. Total volume per batch was 300 ml.

Table A1-1: Paste recipes. Percentages are given per cement weight.

Mix No.	w/b	Silica fume (%)	Filler (%)	Superplasticizer (%)	Stabilizer (%)
1	0.50	0.0	0.0	0.0	0
2	0.50	5.0	0.0	0.0	0
3	0.50	5.0	0.0	1.0	0
4	0.50	0.0	20.0	0.0	0
5a	0.50	5.0	20.0	0.0	0
5b	0.50	5.0	10.0	0.0	0
6	0.50	5.0	20.0	1.0	0
7	0.50	0.0	0.0	0.0	0
8	0.50	0.0	0.0	0.0	1
51	0.50	0.0	0.0	1.0	0
52	0.50	2.5	0.0	2.0	1
53	0.50	5.0	12.5	1.2	0
54	0.50	5.0	0.0	0.8	0
55	0.56	2.5	0.0	2.0	1

Table A1-2: Results – Bingham and Herschel-Bulkley parameters calculated on the whole shear rate range of the down curve (100-1 s^{-1}) for paste and matrix

Mix No.	Bingham Parameters			Herschel-Bulkley Parameters			
	τ_y	μ	R^2	τ_y	K	n	R^2
	[Pa]	[Pa·s]		[Pa]	[Pa·s]		
1	21	0.51	0.94	-0.6	9.09	0.44	1.00
2	118	0.59	0.68	-	-	-	0
3	9	0.13	1.00	8.4	0.18	0.93	1.00
4	103	0.77	0.90	-14.1	32.6	0.32	1.00
5a	49	0.88	0.83	-82.6	145.2	0.12	1.00
5b	64	0.67	0.86	-23.1	57.1	0.20	1.00
6	29	0.21	1.00	30.3	0.09	1.19	1.00
7	38	0.73	0.92	-3.1	19.6	0.4	1.00
8	48	0.73	0.89	-5.7	28.3	0.3	1.00
51	1	0.32	0.99	1.3	0.24	1.01	1.00
52	26	0.10	0.81	-6.8	27.33	0.09	0.95
53	7	0.24	1.00	7.0	0.30	0.96	1.00
54	14	0.26	0.99	11.0	0.88	0.75	1.00
55	17	0.11	0.82	-15.2	25.95	0.10	0.99

Table A1-3: Calculated hysteresis area, flow resistance and gel strengths measured on paste

Mix No.	Hysteresis Area	Flow Resistance	Gel strength 1	Gel strength 2
	[Pa/s]	[Pa/s]	[Pa]	[Pa]
1	662	447	9	33
2	558	2161	91	>250
3	32	178	11	9
4	1511	960	20	100
5a	2692	1976	87	>250
5b	678	1213	41	>250
6	217	554	50	41
7	463	774	13	74
8	2398	921	27	62
51	310	86	0	6
52	254	475	41	50
53	337	185	7	11
54	342	298	14	14
55	190	315	21	27

Development of pumpable mortars

Materials and recipes

The mortars were added 1507 kg/m^3 0-8 mm granitic sand (corresponding to 66 wt%). Apart from that, their compositions were identical to the pastes.

The mixes were proportioned with 400 l/m^3 of matrix and with an estimation of 2 % air. 20 litre batches were mixed to be able to fill the test bucket of the BML (approximately 11 litres) and the slump cone. For most of the mixes, the 0-8 mm sand fraction was used solely. To get even closer to a concrete, the effect of replacing 25 % of the sand with courser aggregate, 4-8 mm sand, was tested. The 0-8 mm sand had a filler content (<125 μm) of 6.3%.

Table A1-4: Mortar recipes. Except for the sand fractions, percentages are given per cement weight.

Mix no.	w/b	Sand 0-8 mm	Sand 4-8 mm	Silica fume	Extra Filler	Super plasticizer	Stabilizer
		[%][1]	[%][1]	[%]	[%]	[%]	[%]
20	0.50	100	0	0	20	0	0
21	0.50	100	0	0	0	1	0
22	0.50	100	0	5	20	1.5	0
23	0.50	100	0	5	0	2	1
24	0.50	100	0	7.5	7.5	2	0
25	0.50	100	0	5	12.5	1	0.5
26[2]	0.50	100	0	0	0	1	0
27	0.50	75	25	0	0	1	0

Experimental

A 50 litre 1980 model Eirich concrete mixer was used for making the 20 l batches. The total mixing time was set to 9 minutes, in order to activate the super plasticizer and to replicate total time as with the mixing sequence for the parallel plate rheometer. The mixing sequence is given in Table A1-5. Note that the shear rate of matrix will be higher in mortar as function of aggregate volume fraction as shown by Wallevik (2003): Typically 4 times higher shear rate in the matrix than in bulk mortar during mixing.

Table A1-5: Mixing sequence

Interval	Duration [s]	Action
1	0-60	Dry mixing
2	60-300	Wet mixing
3	300-420	Resting
4	420-540	Wet mixing
	Σ 9 min	

The rheological properties of the mortar were measured by aid of a BML ConTec Viscometer (BML) and by aid of traditional slump flow measurements. The BML measurement sequence was started 14 min after water addition, and the slump test was carried out approximately 20 min after water addition.

Results

In the following results from the parallel tests, slump, T_{50} and a summary of the BML results are given. The variables, $\geq_y$ and μ, are calculated by using the Reiner-Rivlin equation.

[1] Percent of total amount of sand added.
[2] A new aggregate sieve curve was implemented (incl. 0.4 % abs. water).

Roughly, the T_{50} gives a picture of the plastic viscosity and slump a picture of the yield strength.

Table A1-6: Summarized test results

Mix No.	TWA[3]	Slump	T_{50}	τ_y	μ	Separation	Density
	[min]	[mm]	[s]	[Pa]	[Pa s]	[%]	[kg/m^3]
20	-	0	-	-	-		-
21	-	730	1,4	-4	6,6	29	-
22	-	450	-	-	-	-	-
23	24	600	3,2	18	21.5	20	-
24	20	790	0,9	-4	8.5	20	-
25	22	390	-	108	24.8	8	-
26	22	680	1,2	10	14.7	19	-
27	21	760	0,5	0	8.8	21	2340

Conclusions from the recipe development of mortars

Mixes 51-55 were chosen as a basis for further pumpability experiments as they were regarded the best possible mixes. The compositions of Mix 51-55 are a compromise between obtaining a wide range of rheological properties and at the same time pumpable mortars. It was observed that the differences in rheological properties of pastes made for this study were "diluted" by the addition of aggregates. The relation between reological properties of matrix and mortar is discussed in section 3.2.1 of the report.

[3] TWA – Time after Water Addition.

APPENDIX A2 – Matrix flow curves

In the following, you will find the flow curve for the different mixes. There are also figures of the gel strength, measured by applying a logarithmic increase in shear stress (0-250 Pa) twice with a 10 min rest in between. The break in the curve indicates the gel strength.

MIX 1 – 05 STD FA

This is the No. one reference mix.

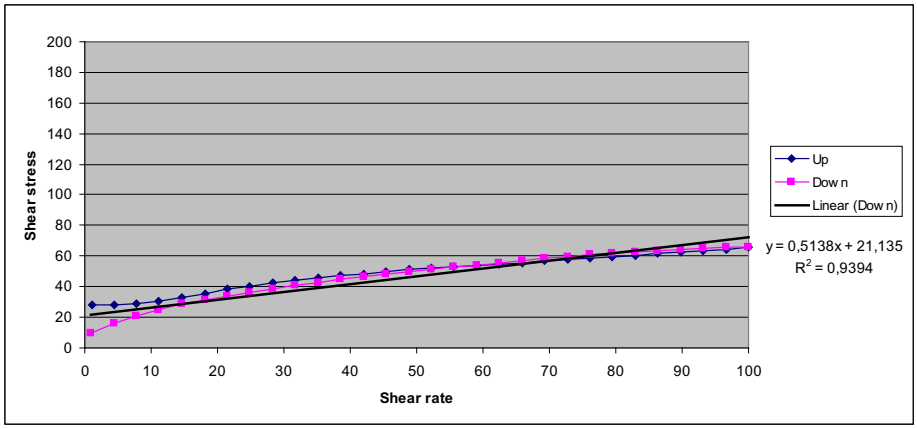

Figure 26 Bingham approach

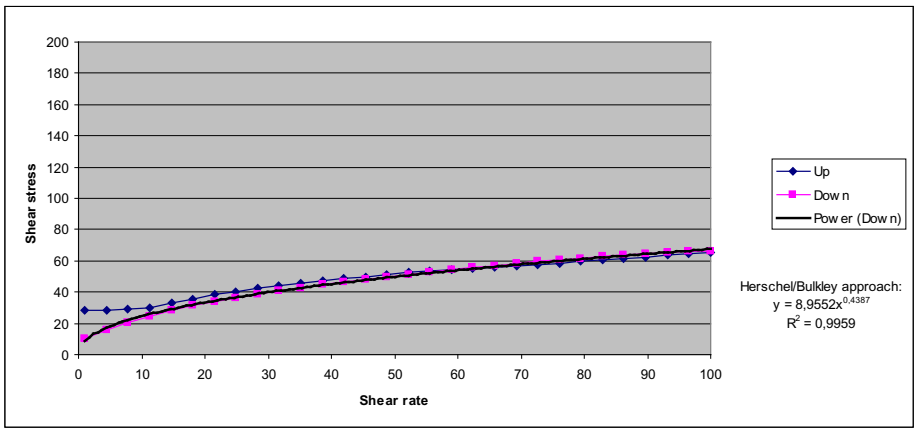

Figure 27 Herschel/Bulkley approach

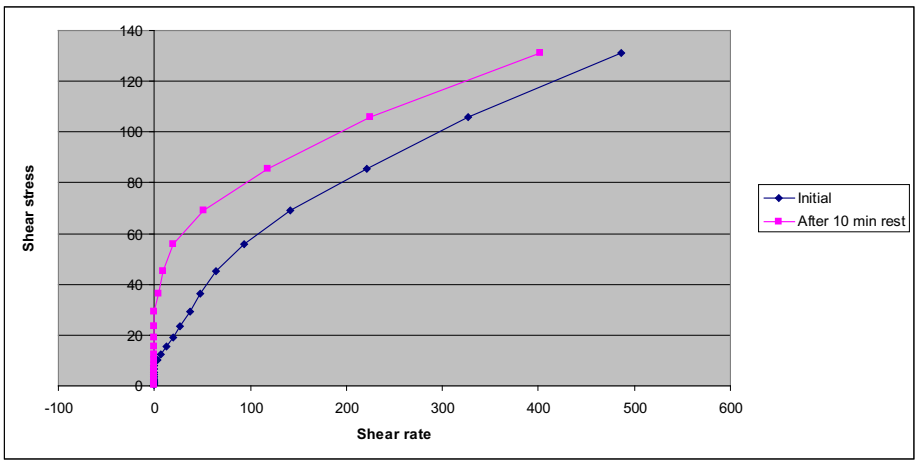

Figure 28 Gel strength - Initial 9 Pa, after 10 min rest 33 Pa

MIX 2 – 05 STD FA 5% S

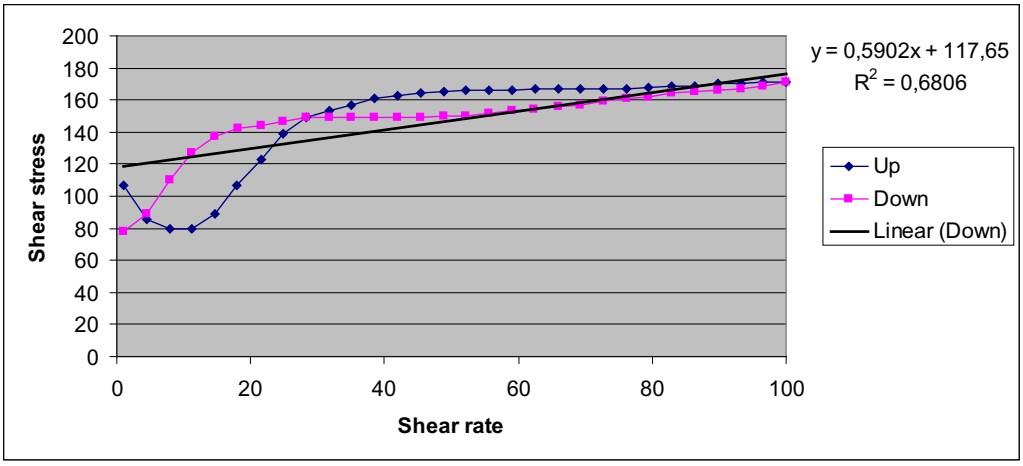

Figure 29 Bingham approach

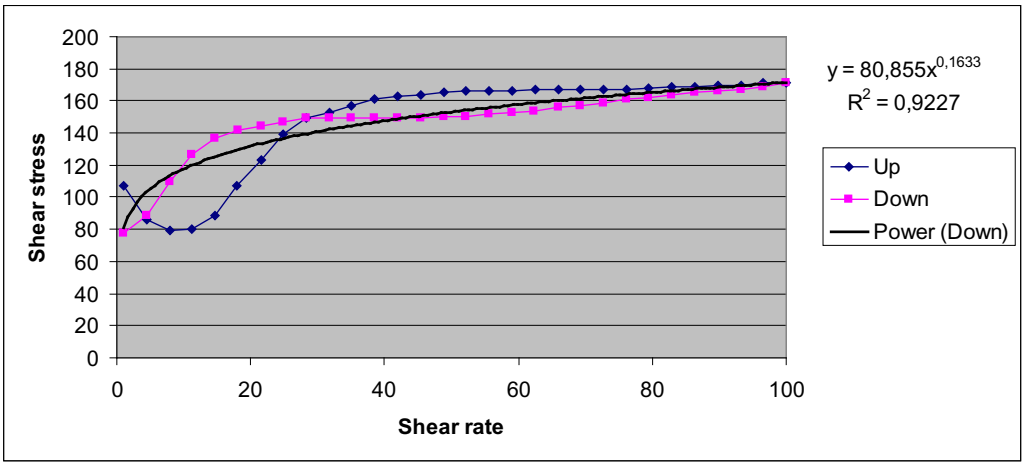

Figure 30 Herschel/Bulkley approach

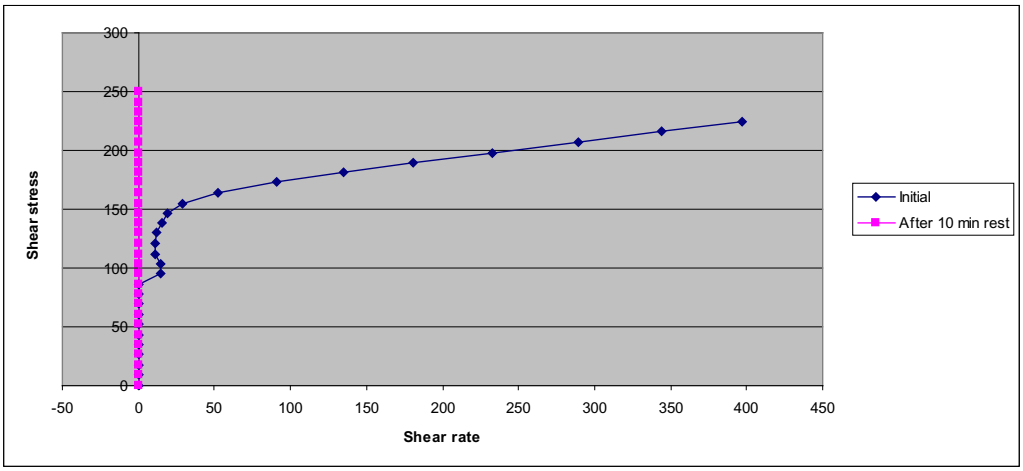

Figure 31 Gel strength – Initial 91 Pa, after 10 min rest >250 Pa.[4]

[4] The gel strength was measured with a linear increase of the shear stress, not a logarithmic as for all the other mixes. I do not though think this influence the results notably.

MIX 3 – 05 STD FA 5 % S 1 % SP

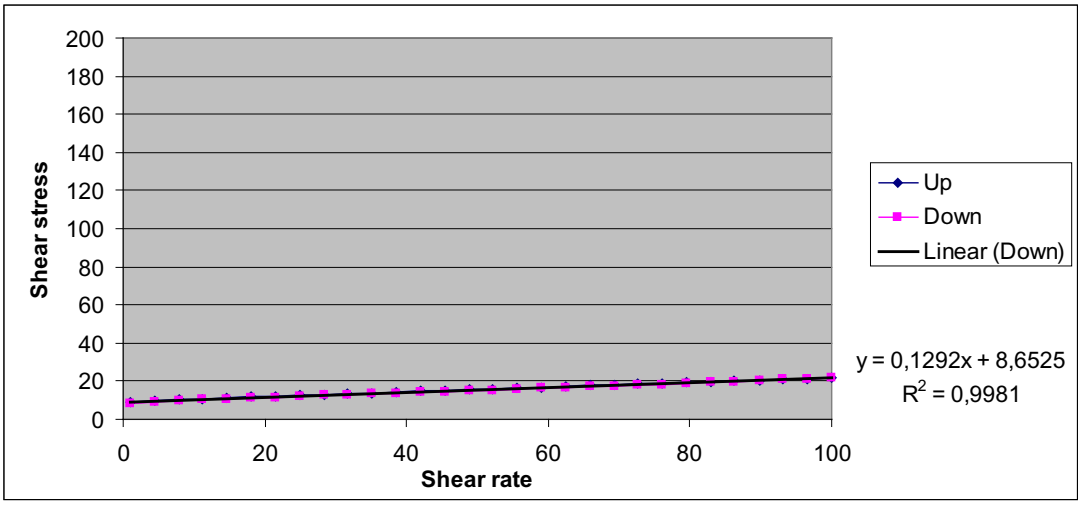

Figure 32 Bingham approach

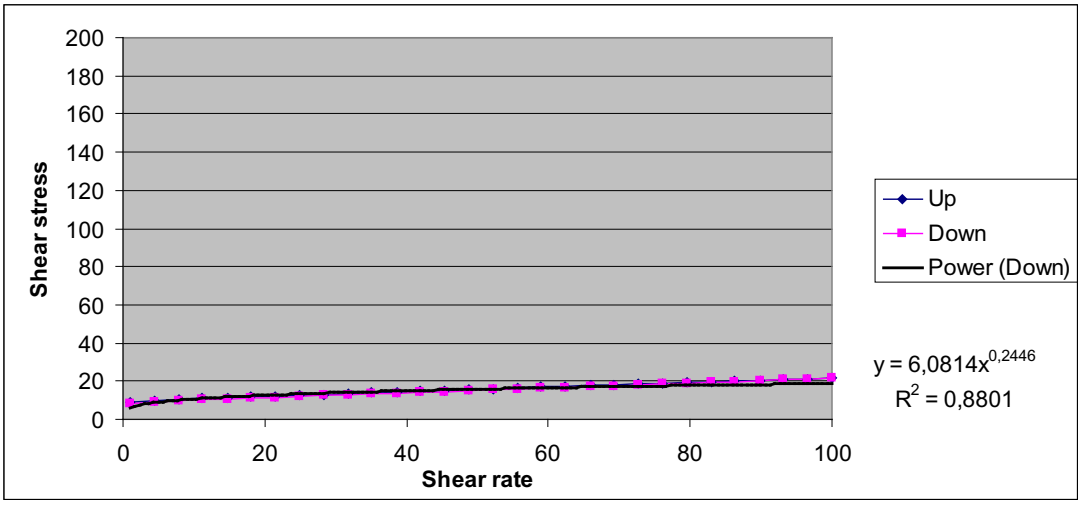

Figure 33 Herschel/Bulkley approach

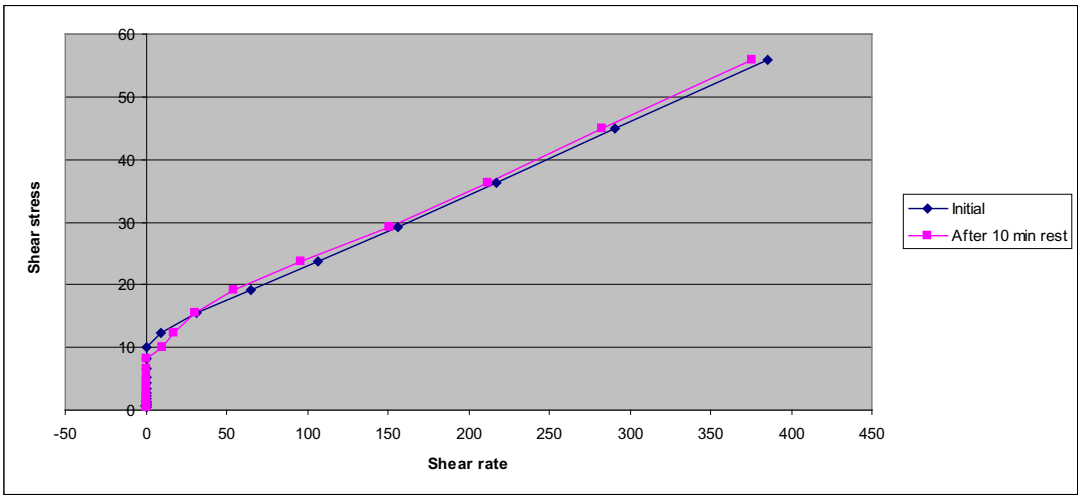

Figure 34 Gel strength - Initial 11 Pa, after 10 min 9 Pa

MIX 4 – 05 STD FA 20% F

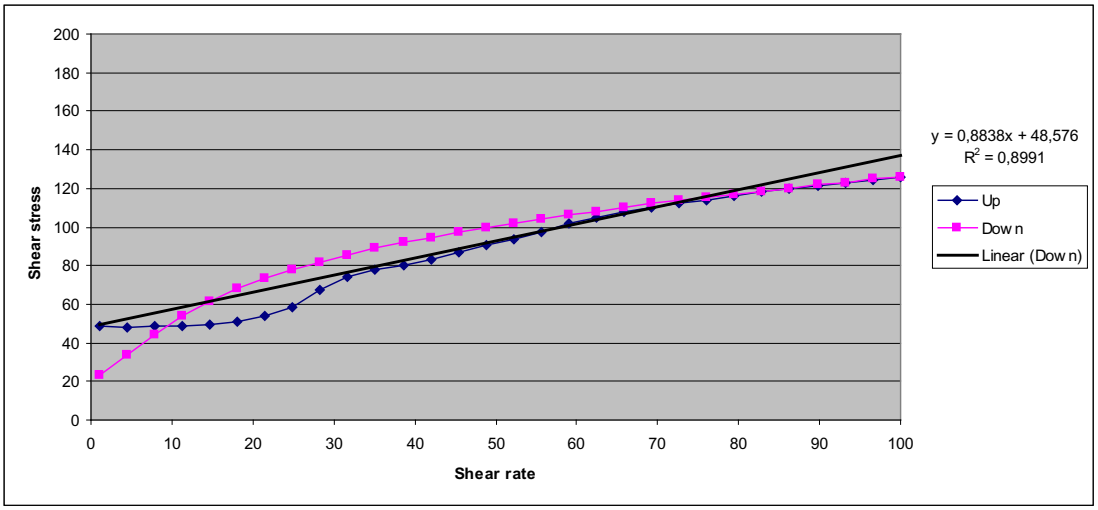

Figure 35 Bingham approach

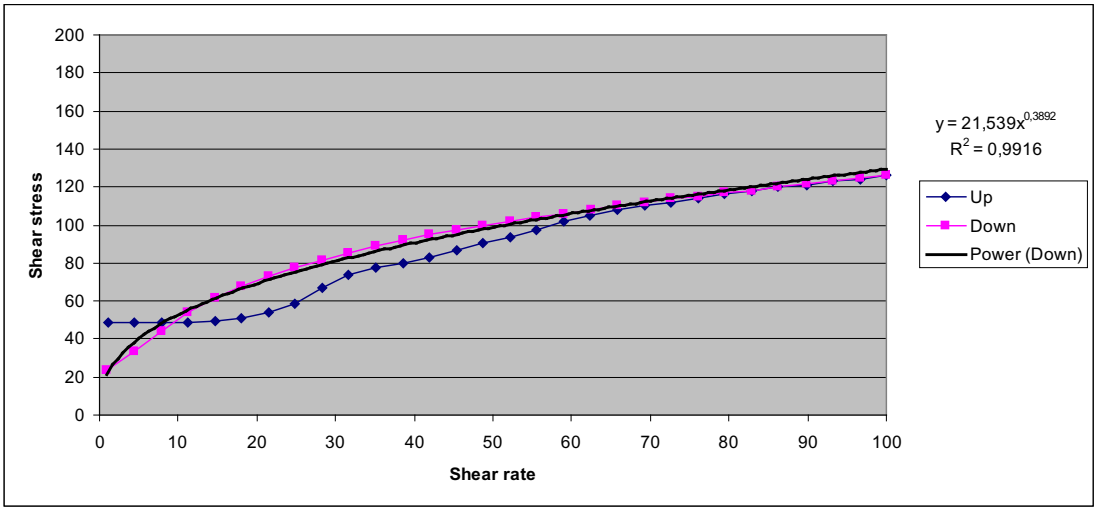

Figure 36 Herschel/Bulkley approach

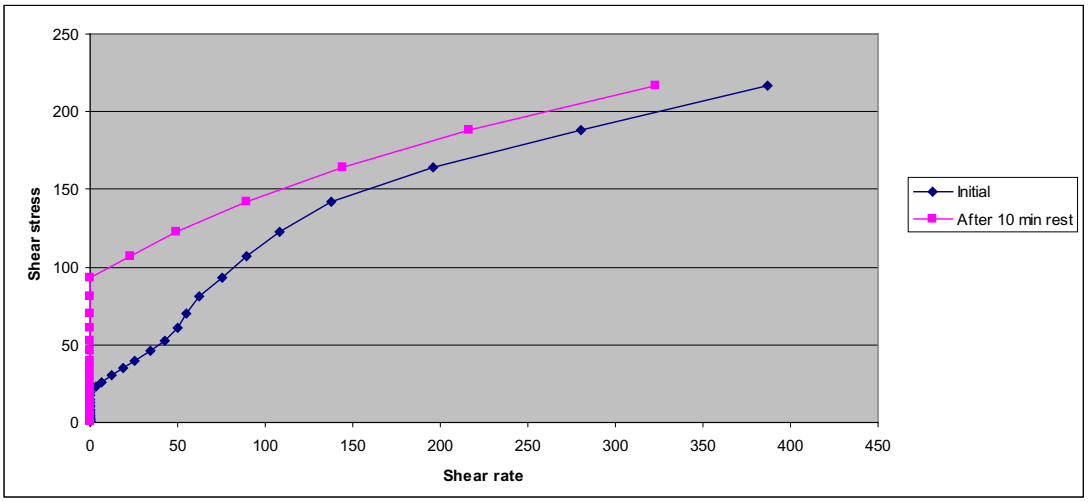

Figure 37 Gel strength – app. 20 Pa initial and app.100 Pa after 10 min.

MIX 5a – 05 STD FA 5% SF 20% F

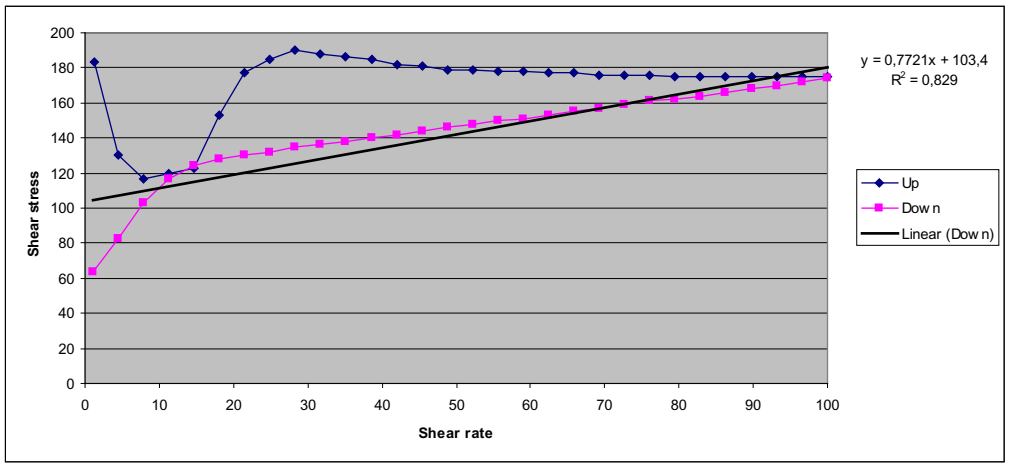

Figure 38 Bingham approach

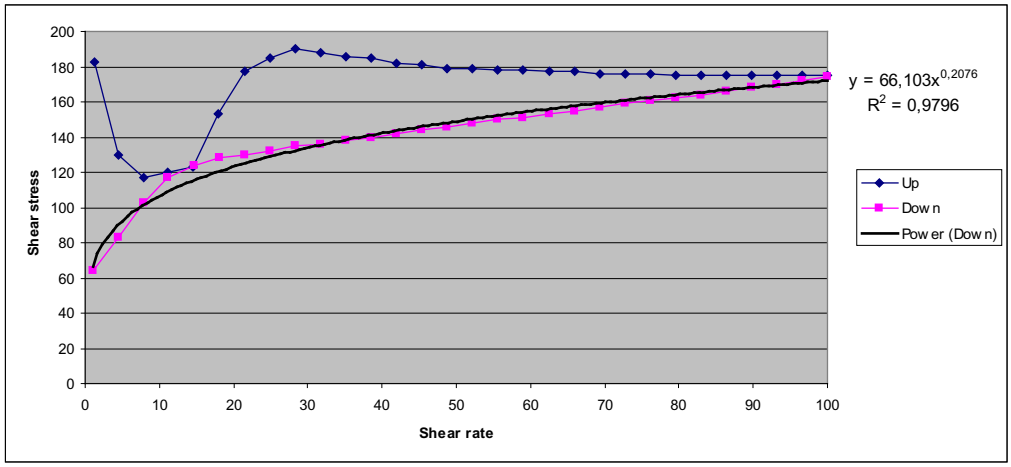

Figure 39 Herschel/Bulkley approach

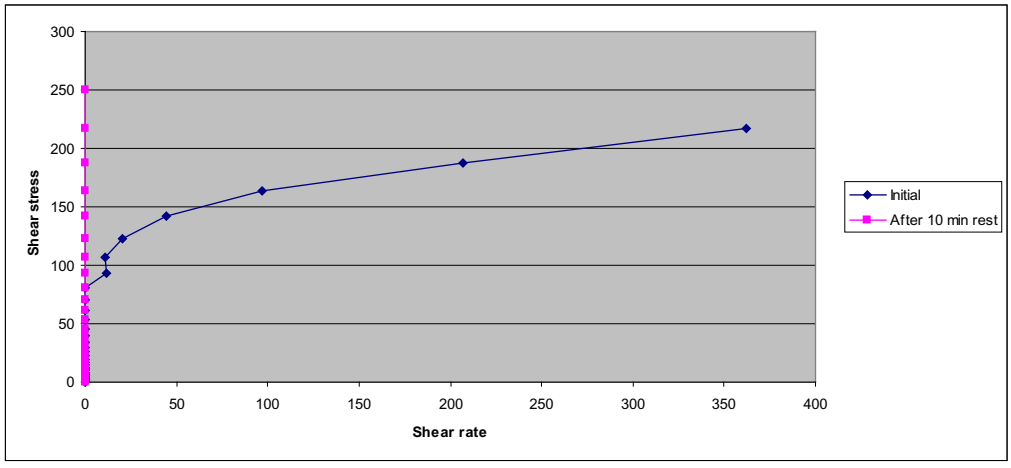

Figure 40 Gel strength - Initial 87 Pa, after 10 min rest >250 Pa.[5]

[5] The gel strength was measured with a linear increase of the shear stress, not a logarithmic as for all the other mixes. This does not influence the results notably.

MIX 5b – 05 STD FA 5% SF 10% F

This mix was made for verifying the incongruous result we got with mix 5a. The only adjustment in the recipe was to reduce the filler content from 20 to 10 %. The results from mix 5b support the results we first got from mix 5a: There is a clear resistance against flow, if we look away from the yield strength, up to approximately 20 Pas. From that level of force and up, the curve follows a more traditional linear path.

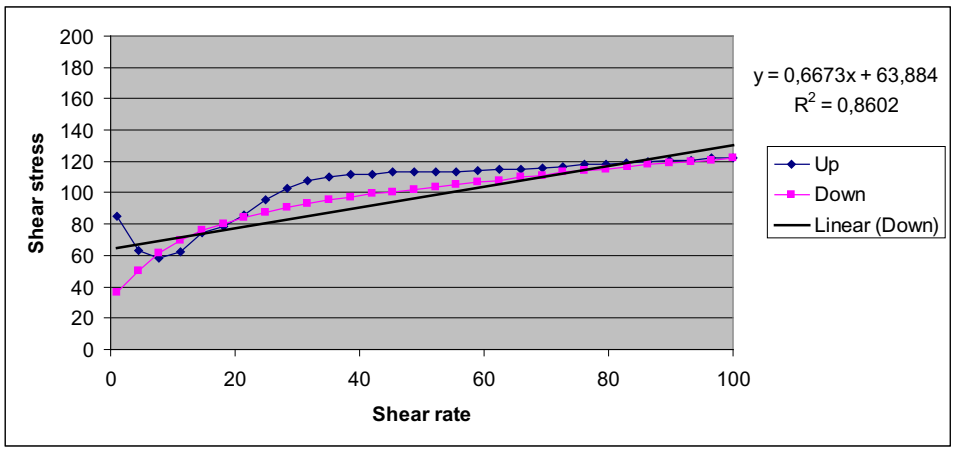

Figure 41 Bingham approach

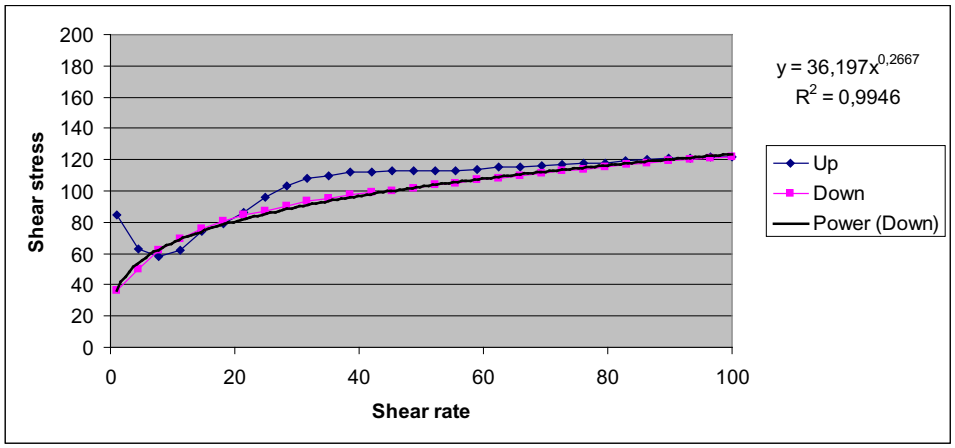

Figure 42 Herschel/Bulkley approach

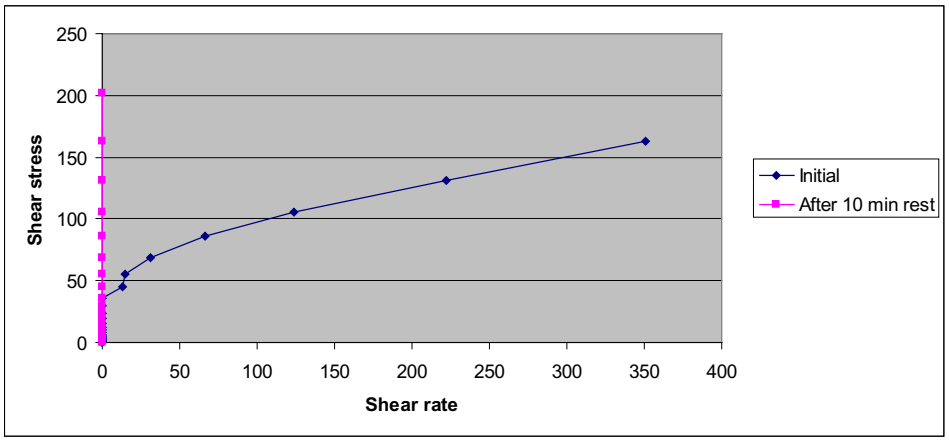

Figure 43 Gel strength- Initial 40 Pa, after 10 min rest >250 Pa.[6]

[6] The gel strength was measured with a linear increase of the shear stress, not a logarithmic as for all the other mixes. This does not influence the results notably.

MIX 6 – 05 STD FA 5% SF 1% SP 20% F

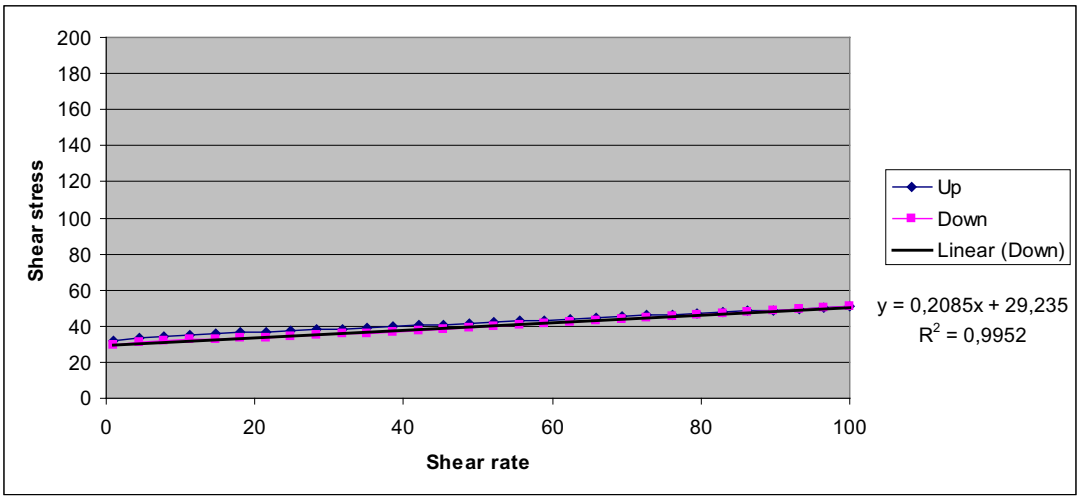

Figure 44 Bingham approach

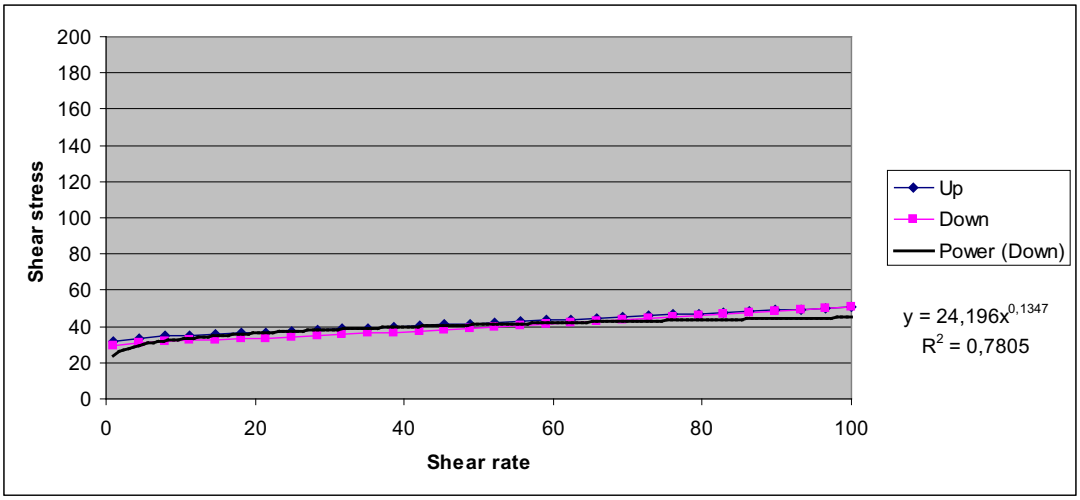

Figure 45 Herschel/Bulkley approach

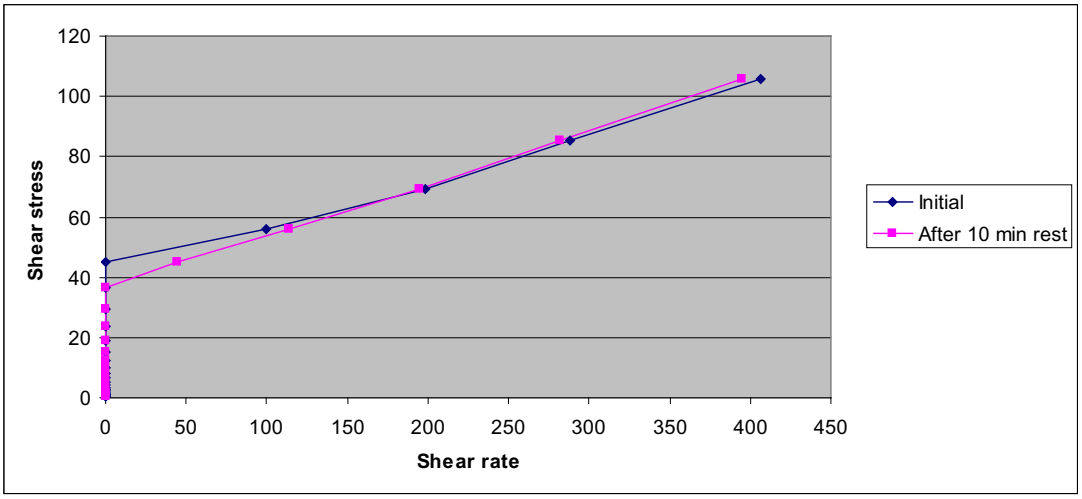

Figure 46 Gel strength - Initial app. 50 Pa and after 10 min rest app. 41 Pa. (We see that the effect of the SP, Glenium 151, increases over time, as the gel strength is reduced after 10 min of resting.)

MIX 7 – 05 STD FA 5% FERROXON

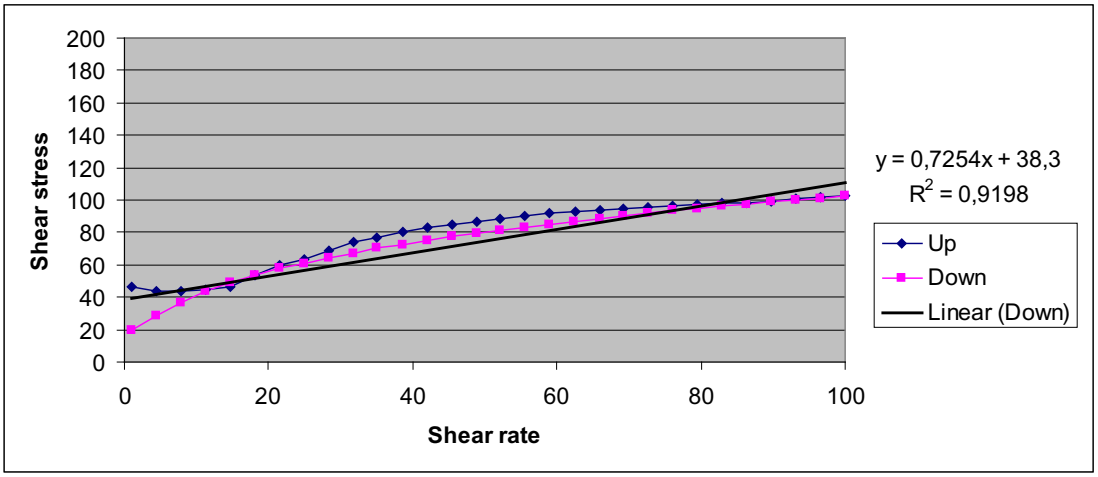

Figure 47 Bingham approach

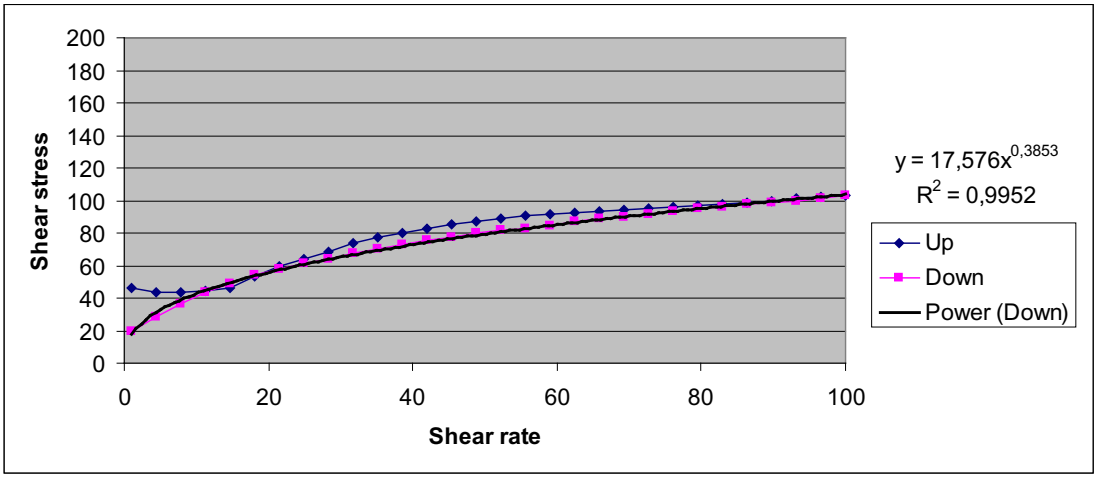

Figure 48 Herschel/Bulkley approach

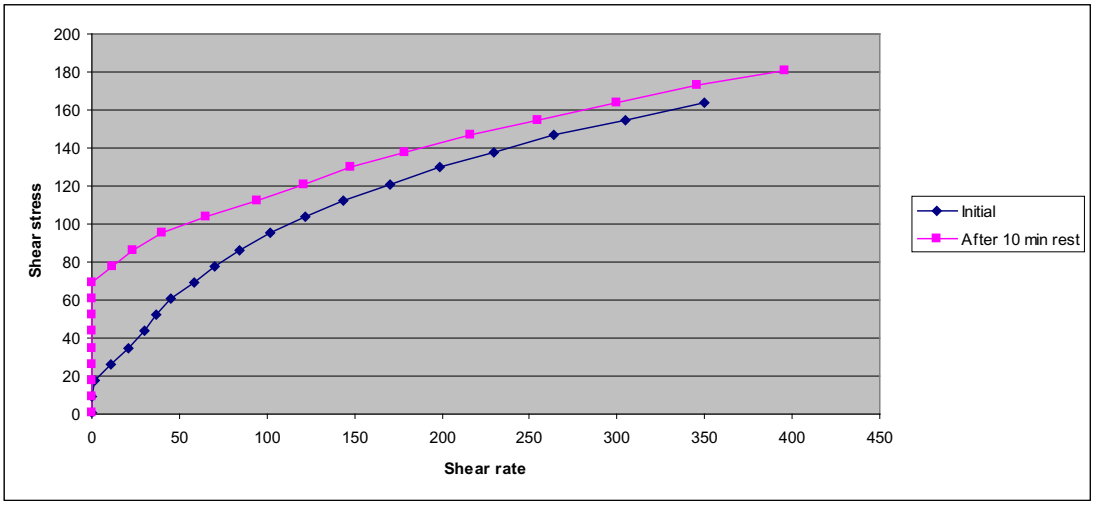

Figure 49 Gel strength - Initial app. 13 Pa, after 10 min app. 74 Pa.[7]

[7] The gel strength was measured with a linear increase of the shear stress, not a logarithmic as for all the other mixes. I do not though think this influence the results notably.

MIX 8 – 05 STD FA 1% STAB

During setting, the paste bled on top of a surface skin.

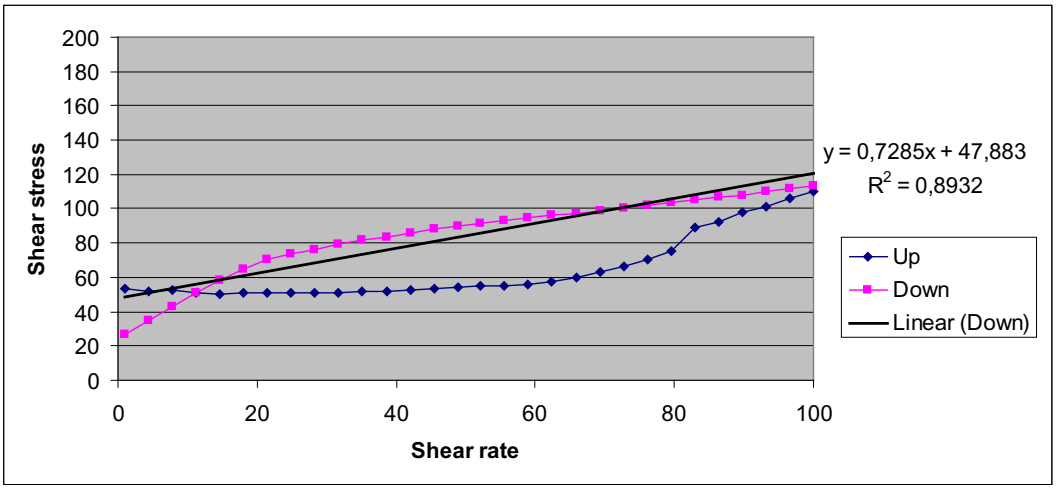

Figure 50 Flow curve - Bingham approach

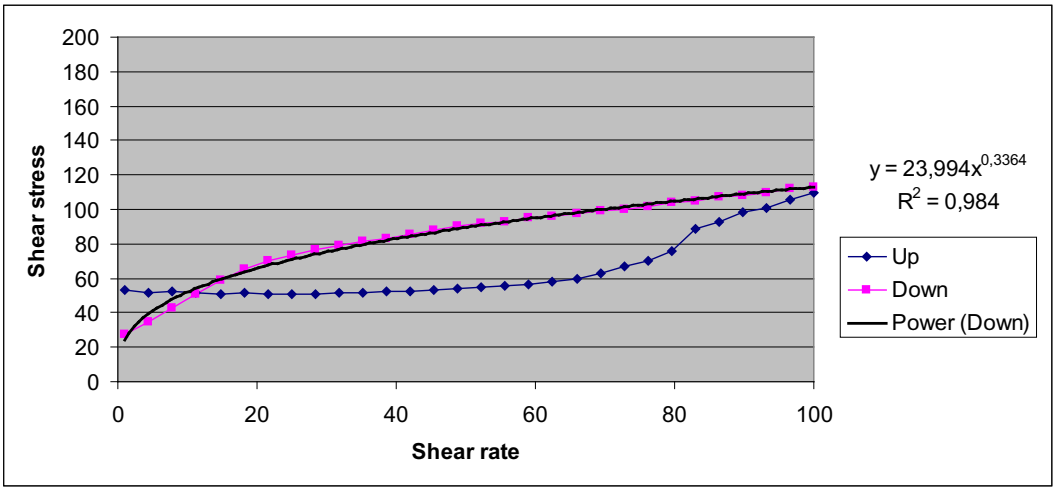

Figure 51 Herschel/Bulkley approach

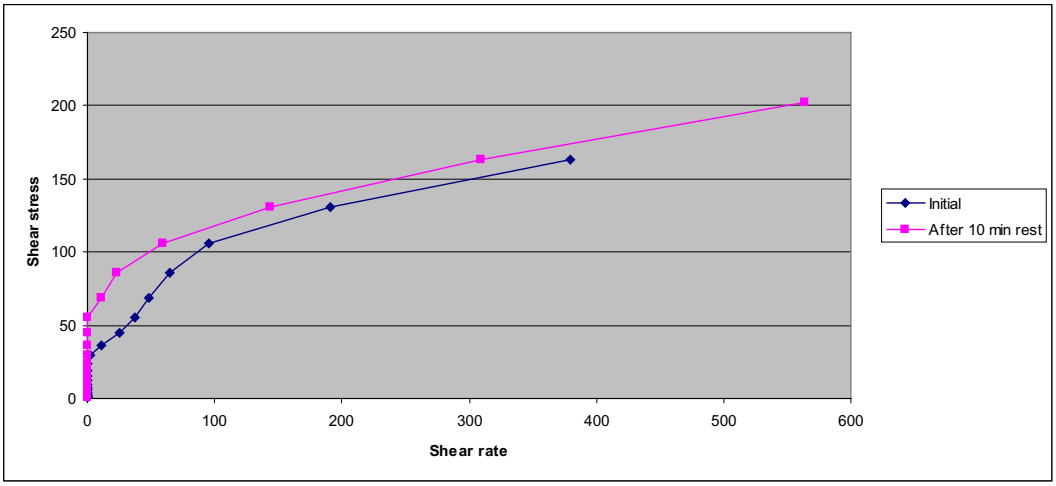

Figure 52 Gel strength - Initial app. 27 Pa, after 10 min app. 62 Pa.

MIX 51 PASTE – 0.50 STD FA 1% SP

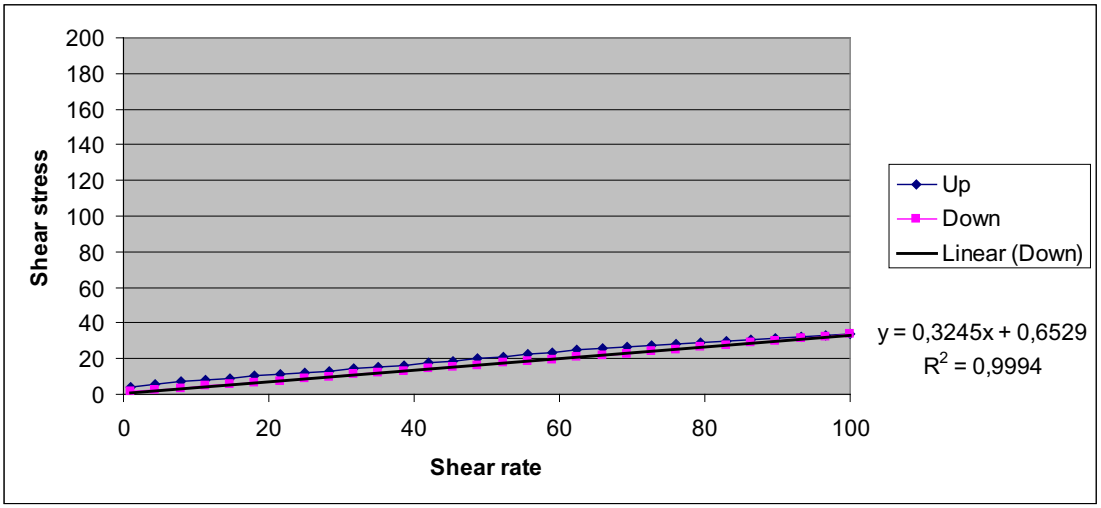

Figure 53 Flow curve - Bingham approach

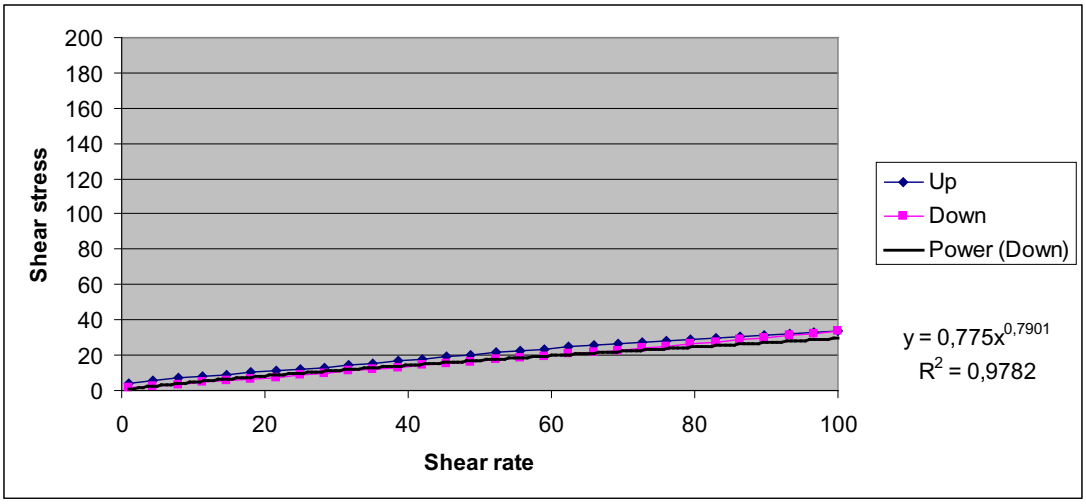

Figure 54 Herschel/Bulkley approach

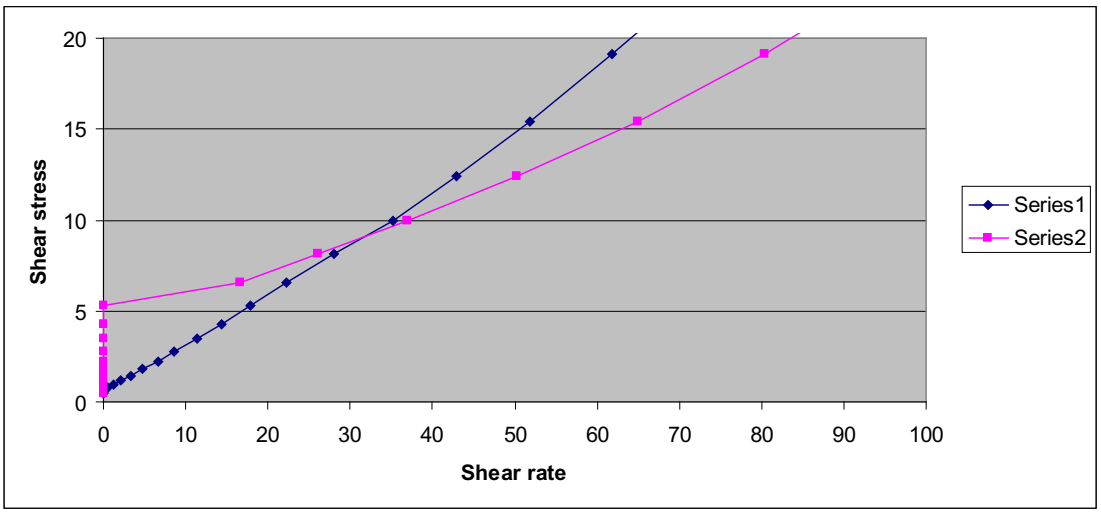

Figure 55 Gel strength - initially 0 Pa, after 10 min rest 6 Pa.

MIX 52 PASTE – 0.50 STD FA 2% SP 2.5% S 1% STAB

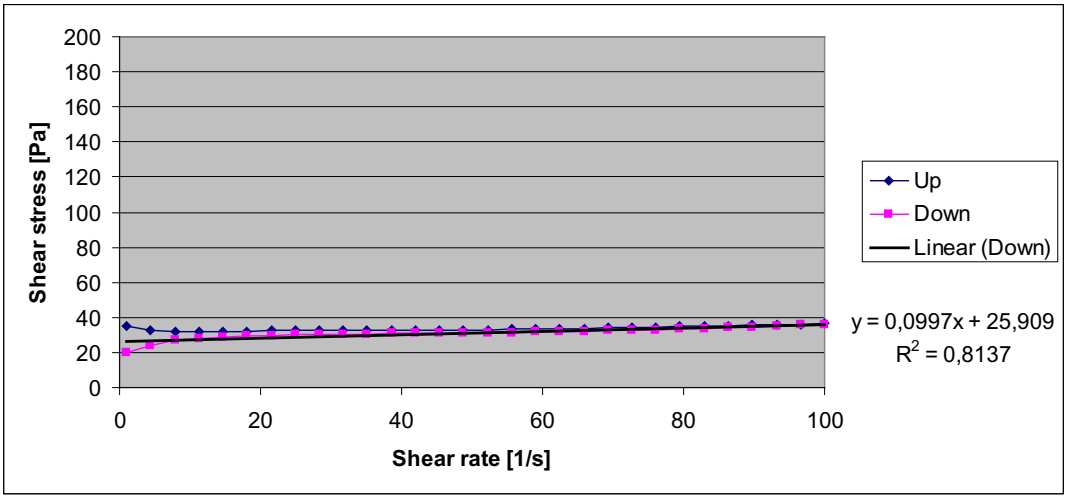

Figure 56 Flow curve - Bingham approach

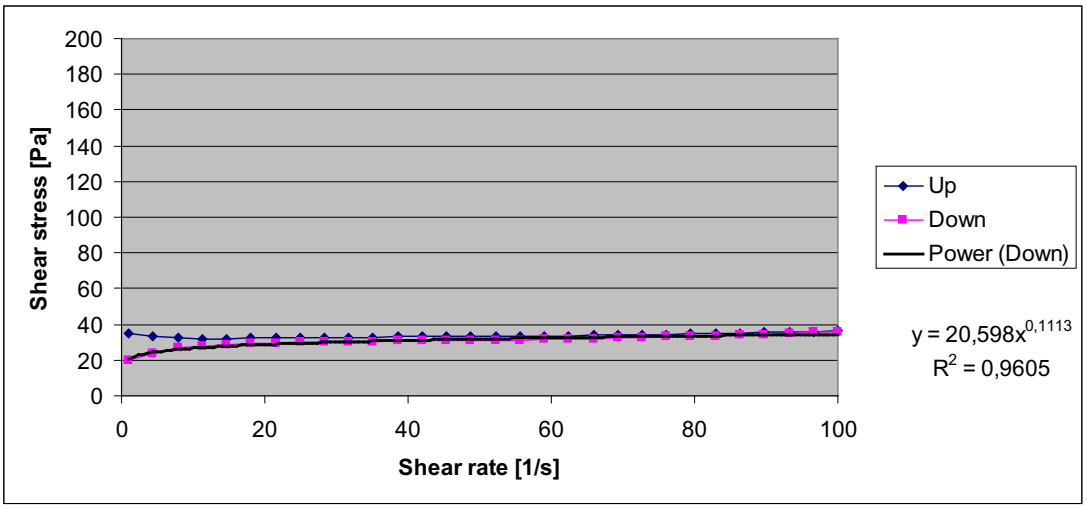

Figure 57 Herschel/Bulkley approach

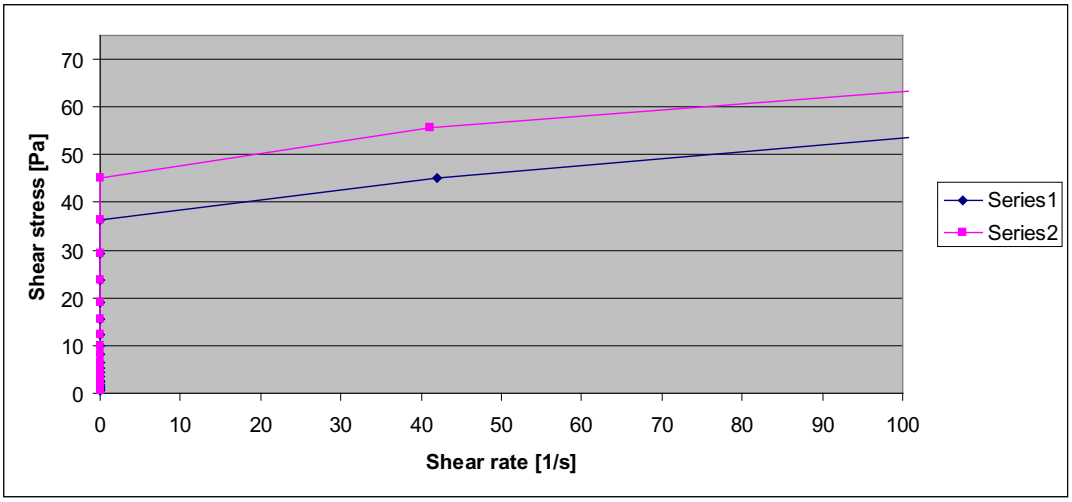

Figure 58 Gel strength – initially 41 Pa, after 10 min rest 50 Pa.

MIX 53 PASTE – 0.50 STD FA 1.2% SP 5% Si 12.5% F

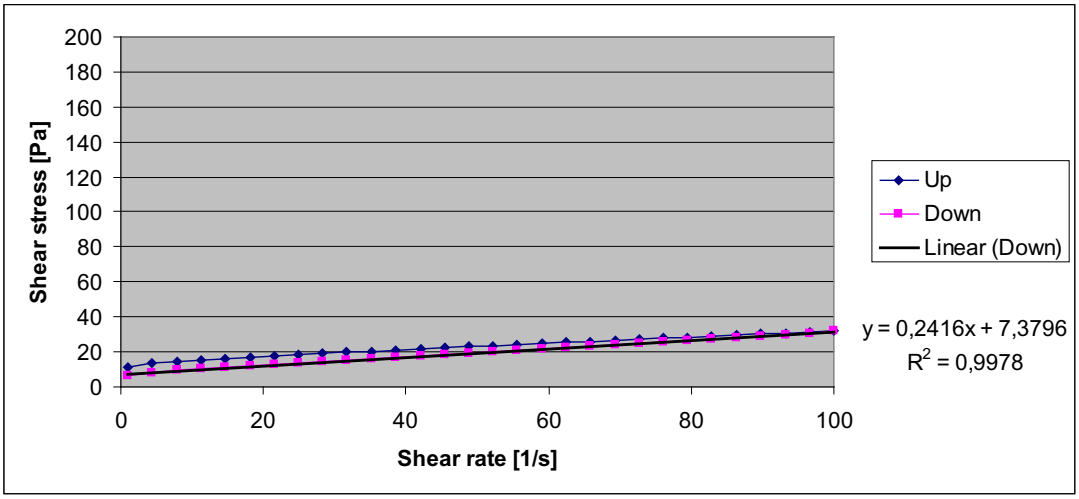

Figure 59 Flow curve – Bingham approach

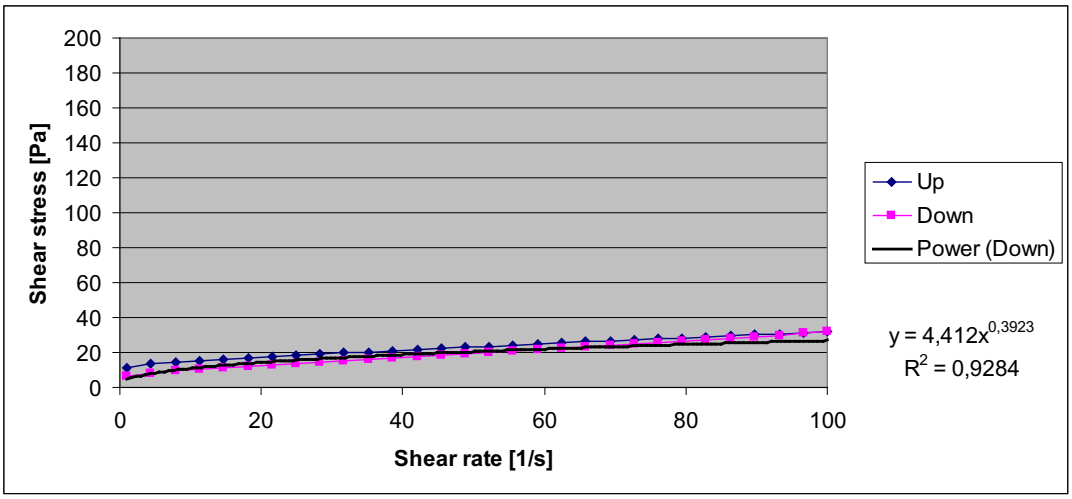

Figure 60 Herschel/Bulkley approach

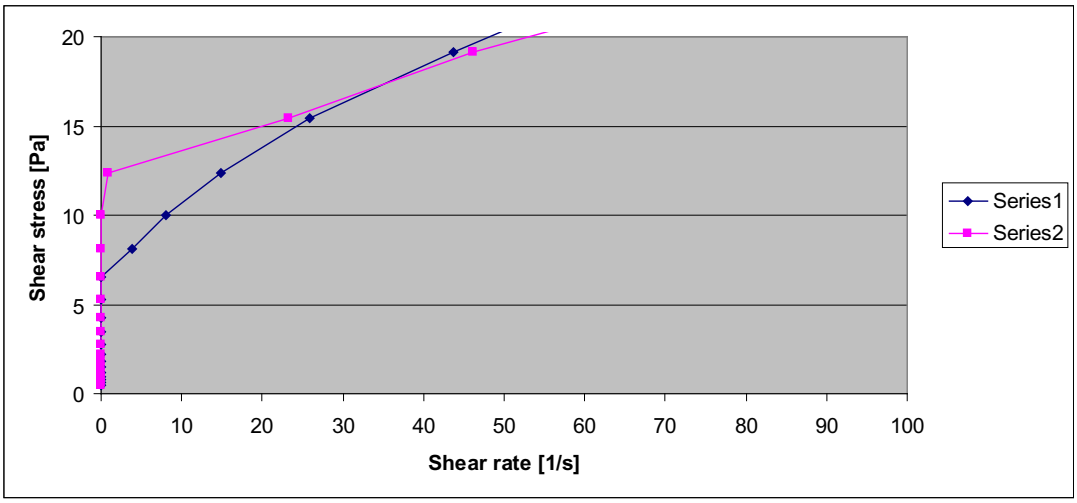

Figure 61 Gel strength – initially 7 Pa, after 10 min rest 11 Pa.

MIX 54 PASTE – 0.50 STD FA 2% SP 2.5% S 1% STAB

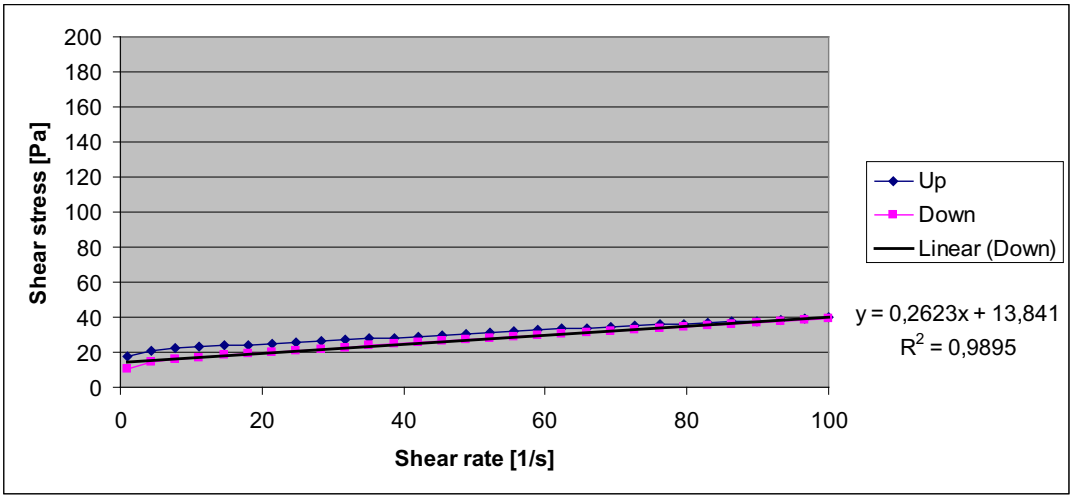

Figure 62 Flow curve – Bingham approach

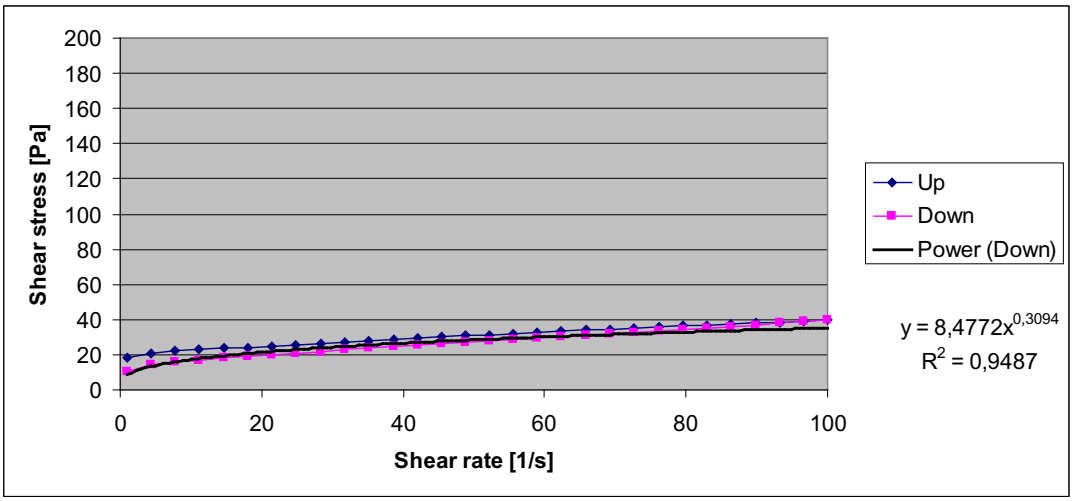

Figure 63 Herschel/Bulkley approach

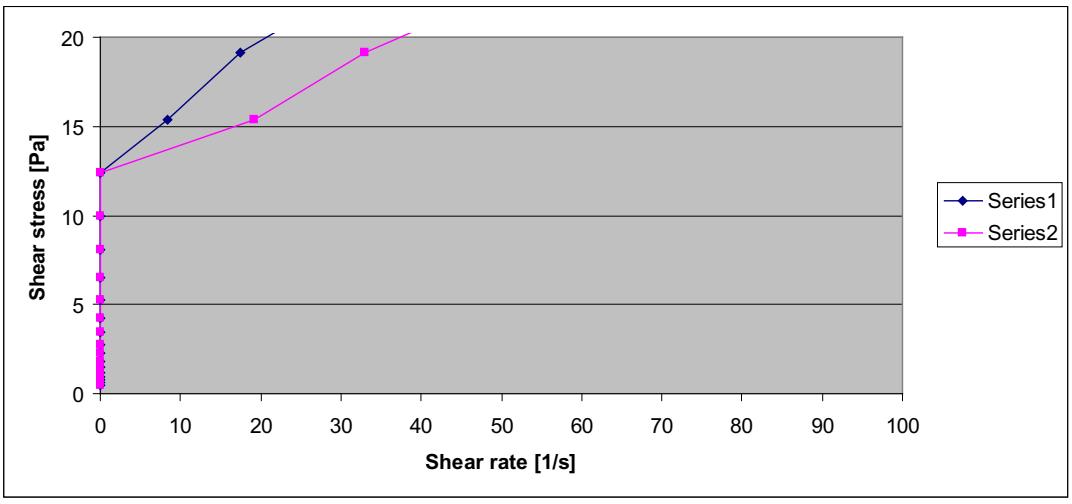

Figure 64 Gel strength – initially 14 Pa, after 10 min rest 14 Pa.

MIX 55 PASTE – 0.50 STD FA 2% SP 2.5% S 1% STAB

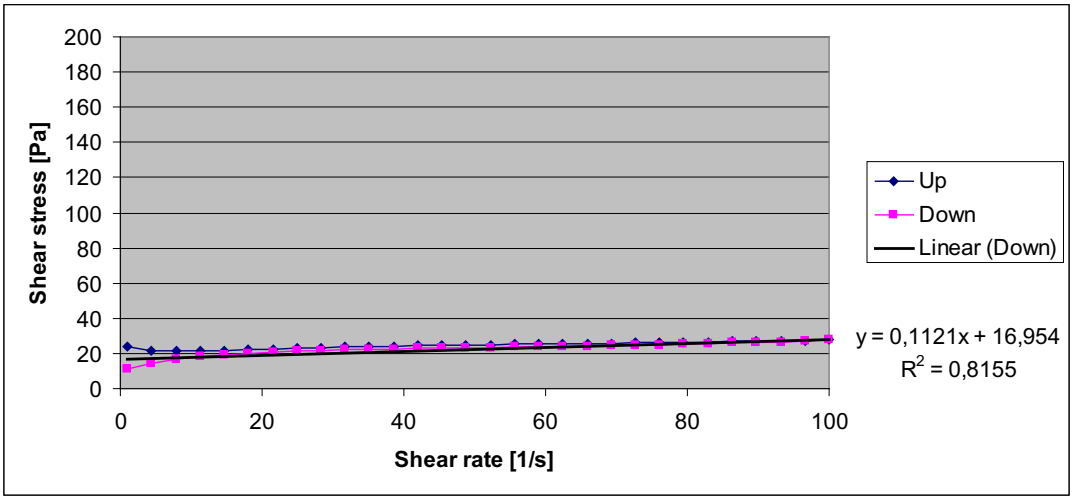

Figure 65 Flow curve – Bingham approach

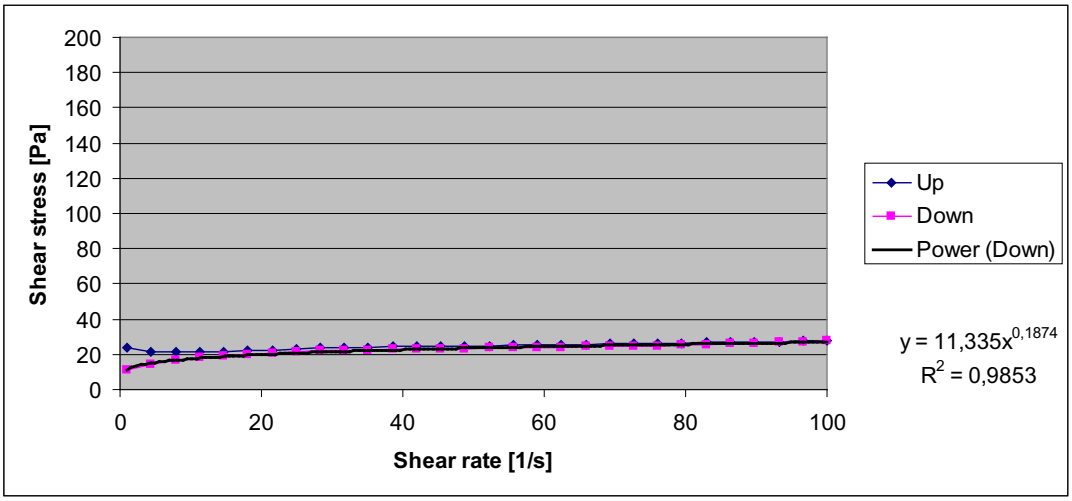

Figure 66 Herschel/Bulkley approach

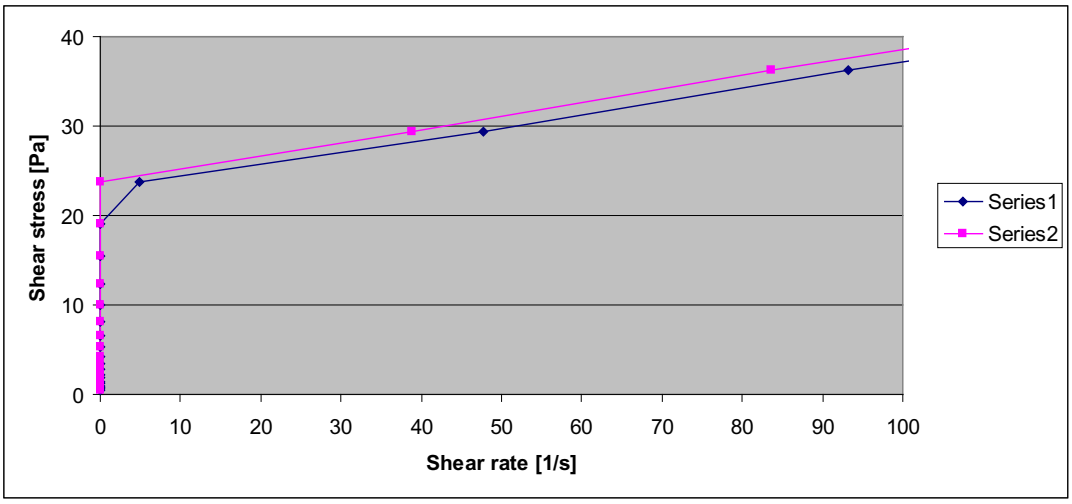

Figure 67 Gel strength – initially 21 Pa, after 10 min rest 27 Pa.

APPENDIX A3 – Plug profiles of pumped concrete

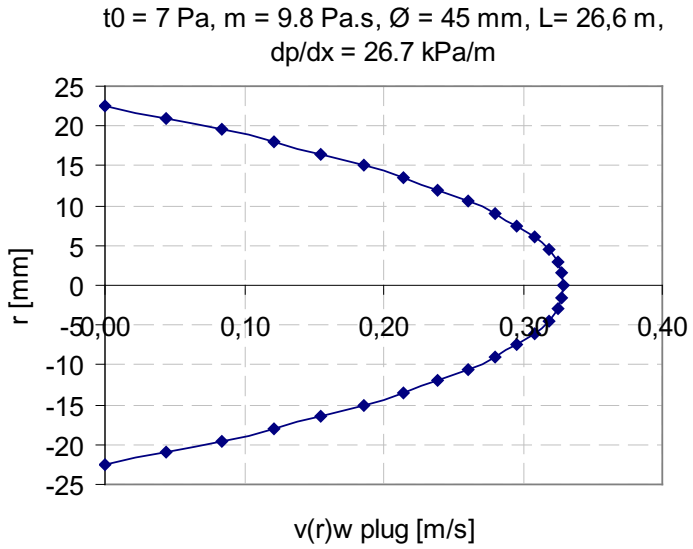

Figure A3-1: Example of simulated plug calculated with Buckingham-Reiner for Mix 51, pumped at 50 Hz.

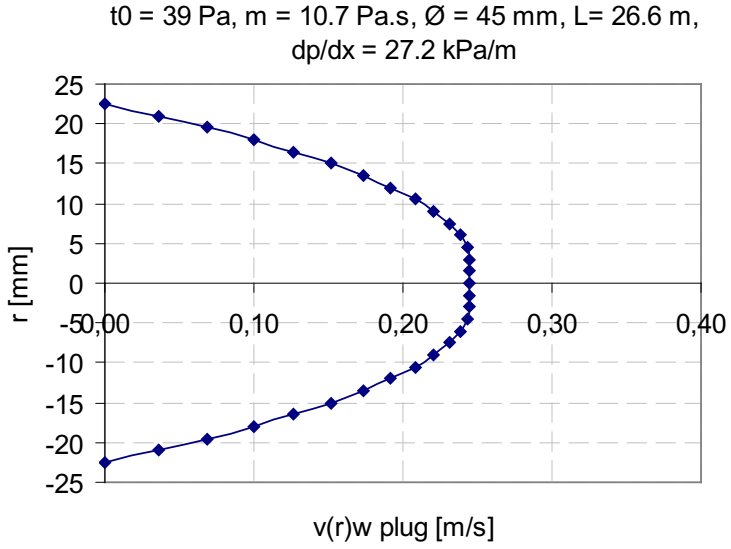

Figure A3-2: Mix 53; Buckingham-Reiner, pumped at 50 Hz.

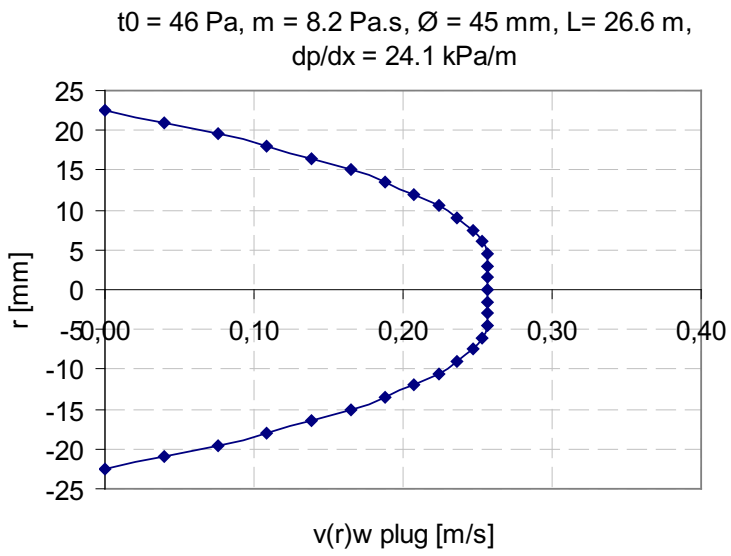

Figure A3-3: Mix 54; Buckingham-Reiner, pumped at 50 Hz.

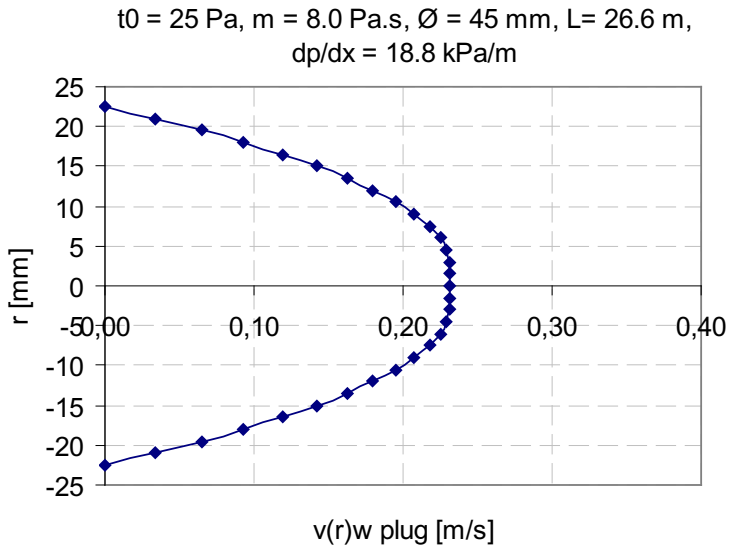

Figure A3-4: Mix 55; Buckingham-Reiner, pumped at 50 Hz.

SINTEF Building and Infrastructure is the third largest building research institute in Europe. Our objective is to promote environmentally friendly, cost-effective products and solutions within the built environment. SINTEF Building and Infrastructure is Norway's leading provider of research-based knowledge to the construction sector. Through our activity in research and development, we have established a unique platform for disseminating knowledge throughout a large part of the construction industry.

COIN – Concrete Innovation Center is a Center for Research based Innovation (CRI) initiated by the Research Council of Norway. The vision of COIN is creation of more attractive concrete buildings and constructions. The primary goal is to fulfill this vision by bringing the development a major leap forward by long-term research in close alliances with the industry regarding advanced materials, efficient construction techniques and new design concepts combined with more environmentally friendly material production.